PONTIFICIA UNIVERSIDAD CATÓLICA DE CHILE
ESCUELA DE INGENIERÍA

THERMODYNAMIC STUDY OF THE EXTRACTION OF GUAIACOL FROM HYDROCARBONS FOR BIO-OIL UPGRADE

MATÍAS IGNACIO CAMPOS FRANZANI

Thesis submitted to the Office of Research and Graduate Studies
in partial fulfillment of the requirements for the degree of
Master of Science in Engineering

Advisor:
ROBERTO CANALES

Santiago de Chile, April 2020

PONTIFICIA UNIVERSIDAD CATÓLICA DE CHILE
ESCUELA DE INGENIERÍA

THERMODYNAMIC STUDY OF THE EXTRACTION OF GUAIACOL FROM HYDROCARBONS FOR BIO-OIL UPGRADE

MATÍAS IGNACIO CAMPOS FRANZANI

Members of the Committee:
ROBERTO CANALES
NÉSTOR ESCALONA
RICARDO PÉREZ
JUAN DE LA FUENTE
MARCELO ARENAS

Thesis submitted to the Office of Research and Graduate Studies in partial fulfillment of the requirements for the degree of Master of Science in Engineering

Santiago de Chile, April 2020

Dime y lo olvido, enséñame y lo
recuerdo, involúcrame y lo aprendo

ACKNOWLEDGEMENTS

First of all, I want to thank to my friends who worked with me and they help me to keep going all the time.

I would also like to thank Dr. Roberto Canales, my advisor, for your great help and advice that helped me to be the professional that I am.

My greatest thanks goes to the students who helped me realize one of my greatest vocations, teach.

Finally I would like to thank the financial support from Dr. Néstor Escalona, director of the Nucleo Milenio en Procesos Catalíticos hacia la Química Sustentable.

TABLE OF CONTENTS

LIST OF FIGURES

LIST OF TABLES

ABSTRACT

Within the last decade, fossil fuels have been exploited to obtain an energy source and be the basis in the synthesis of many products. On the other hand, this type of fuel has a high carbon footprint and is not reusable, which makes it less selective every day. That is why, renewable resources have been studied for years. One of the most studied is fuel biomass, which is understood as any mixture of organic compounds, which can be used for new industrial processes.The most abundant compounds in vegetable biomass is lignin, which is found mainly in wood. This compound can be the raw material of various processes, highlighting pyrolysis, which treats lignin at temperatures above 200 and up to 370 ^{o}C, obtaining a liquid called bio-oil. Bio-oil is a mixture of several organic compounds, which serve as raw material for the synthesis of various products or as a fuel. In the case of this study, guaiacol will be used as an ideal model of the oil obtained. The main objective is to characterize the possible solvents that can be used to carry out future synthesis or extractions from the bio-oil. Different properties were calculated to understand the thermodynamic behavior of the mixtures and balances as appropriate. In addition, behaviors will be modeled to be able to extrapolate to different situations and thus have a broad spectrum in which one can work.

Solvents that form only one phase with guaiacol, were determined, which were methanol, ethanol and acetone. On the other hand,those that form liquid-liquid equilibria were also determined, which were dodecane and hexadecane. Finally, the different properties and behaviors were modeled with different models, reaching concrete results that lay the foundations for upcoming research.

Keywords: excess volume, mixture viscosity, mixture density, liquid-liquid equilibria, thermodynamic models.

RESUMEN

Dentro de la última década, los combustibles fósiles han sido explotados para obtener una fuente de energía y ser la base en la síntesis de diversos productos. Este tipo de combustibles presentan una alta huella de carbono y no son reutilizables, lo que los hace cada día menos atractivos. Es por esto, que hace algunos años se están estudiando fuentes renovables, como posibles alternativas. Una de las principales es la biomasa, que se entiende como cualquier mezcla de compuestos orgánicos, la cual puede ser aprovechada para nuevos procesos industriales. Dentro de los compuestos más abundantes en la biomasa, se encuentra la lignina, la cual se encuentra principalmente en la madera. Este compuesto puede ser la materia prima de diversos procesos, destacándose la pirólisis, que trata a la lignina a temperaturas sobre los 200 y hasta los 370 ^{o}C, obteniéndose un líquido llamado bio-oil. El bio-oil es una mezcla de varios compuestos orgánicos, los cuales sirven como precursores para la síntesis de diversos productos o como combustible. Para el caso de este estudio se utilizará el guaiacol como modelo ideal del aceite obtenido. El principal objetivo es caracterizar los posibles solventes que puedan servir para realizar futuras síntesis o extracciones a partir del bio-oil. Para esto, se calcularon diferentes propiedades que permitan entender el comportamiento termodinámico de las mezclas y equilibrios según corresponda. Además, se modelaron los comportamientos para poder extrapolar a distintos escenarios y así tener un gran espectro en el cual se pueda trabajar.

Se logró determinar que el metanol, etanol y acetona son los solventes que forman solo una fase con el guaiacol, y los que formaron equilibrio líquido-líquido, dodecano y hexadecano. Finalmente, se logró modelar de buena manera las diferentes propiedades, pudiendo explicar el comportamiento de los equilibrios en estudio.

Palabras Claves: volumen de exceso, viscosidad de mezcla, densidad de mezcla, equilibrio líquido-líquido, modelos termodinámicos.

1. INTRODUCTION

The abundance of cheap fossil fuels like coal and petroleum created a cheap energy source. However, this dependence on fossil fuels seems to act negatively in the sustainable growth of human society and economy. In order to keep up with a sustainable industrial and economic growth, new sources of energy products had to be explored. The production of biomass-based fuels and chemicals has the potential to be a cost-effective and environmentally friendly solution to this problem. The great diversification that biomass has had in recent years has been a key factor to invest in these new technologies that allow converting this raw material into products with high added value.

One of the goal of the research is to allow biomass to be taken into account as a substitute for oil. This means that multiple products can be produced from it. Similar to the traditional refinery, the biorefinery uses the principles of the traditional one that through different processes convert the different types of biomass into multiple products that were previously synthesized from petroleum (Demirbas, 2009).

There are some reasons why it is attractive to study biomass as a source of energy and as a synthesis of high value products. First of all, it is sustainable, renewable and has a low environmental footprint (Verma et al., 2012). On the other hand, in the last decade the price of oil has proven to be unstable, making it difficult to estimate resources and production. When the demand for oil is high and the oil supply is going down, the use of biomass can be a good alternative as a substitute for the lost supply.

Biomass is composed of several compounds, for example carbohydrates, lignin, fats and proteins (Verma et al., 2012). The characteristics of the biomass vary according to the source. The source can be any vegetable, such as plants, crop waste or any biocomposite that you want to dispose of (Verma et al., 2012). This is why, in addition to being a source

for synthesizing new compounds, it is a way to reduce waste. The resulting biomass conversion products are dependent on the source of the biomass and also on the transformation process (liquid, gas or solid).

Lignin is considered one of the most interesting biomass resources to be processed to produce biofuels and chemicals such as phenolics (Upton & Kasko, 2015). Lignin has a complex structure and is found mainly in wood (Lamsal & Tyagi, 2010). It is a byproduct of the paper industry and can now be burned to produce energy. This practice is not recommended because it generates polluting gas emissions. Many different processes for the conversion of lignin into fuel and chemicals are being studied. Some of them are pyrolysis, hydrothermal conversion, electrochemical degradation, enzymatic or catalysed degradation and others (Kang, Li, Fan, & Chang, 2013).

Lignin is commonly treated with a hydrothermal process, which produces three main products. For temperatures lower than 200 ^{o}C the process is called hydrothermal carbonization and the product is a hydrochar which can be compared with low rank coal (Elliott, Biller, Ross, Schmidt, & Jones, 2015). At temperatures between 200 and 370 ^{o}C, the process is called hydrothermal liquefaction and the product is liquid fuel (biocrude) (Peterson et al., 2008). Biocrude resembles petroleum and can be upgraded to the same range of fuel products. At temperatures above 370 ^{o}C the process becomes a hydrothermal gasification which produces a synthetic fuel gas (syngas) (Peterson et al., 2008).

This work focuses on the liquid product obtained from the rapid pyrolysis of lignin, this product is known as bio-oil. Which is treated in a catalytic process to obtain multiple compounds, within which the phenols stand out. Specifically, this work will address the study of guaiacol, a compound used as a bio-oil model, due to the presence of oxygenated functions. The hydrodeoxygenation of guaiacol generates a large number of products with various sub products and pathways (Silva, Ribas, Monteiro, de Souza Barrozo, & Soares, 2020). The most important products are phenolic compounds such as phenol and

cresol, aromatic hydrocarbons such as toluene and benzene and methoxy ethers as anisole (Sulman et al., 2019). Usually the catalytic hydrodeoxygenation of guaiacol is carried out on long chain hydrocarbons such as decane, dodecane or hexadecane (Blanco et al., 2019). Due to the differences in molecular composition and the wide variety of functional groups that are present in the reaction, the separation of these compounds after the reaction can be a challenge.

Dodecane and hexadecane are typical solvents for heterogeneous catalyzed reactions when the reactants are lignin derivatives. Therefore, for studying an effective separation process of the guaiacol from the solvent, it is necessary an initial knowledge on thermodynamic, physicochemical, and transport properties of the binary mixtures involved before analyzing the real multicomponent mixture. Experimental measurements can validate the models used for representing these systems in process simulations performed as the first stage for designing practical applications.

In this work density, dynamic viscosity, binary liquid-liquid equilibrium if present, for mixtures of guaiacol + dodecane, guaiacol + hexadecane, guaiacol + methanol and guaiacol + ethanol and guaiacol + acetone over the entire range of concentrations for different temperatures and ternary liquid-liquid equilibria, were measured. Also, excess properties were calculated using mixture densities in order to explain the molecular interactions between components in the non-ideal system. These results of density and excess volume have been modeled with PC-SAFT equation of state, dynamic viscosity have been modeled with VFT model and liquid-liquid equilibrium have been modeled with Cosmo RS, Cosmo SAC and PC-SAFT.

1. Goals

The main objective of this work is to present and show the thermodynamic behavior of the mixture of guaiacol with the hexadecane and dodecane and find the best solvent to separate them for future reactions or syntheses. To achieve this, the following specific goals are proposed:

(i) Study and model the density, excess volume and dynamic viscosity of completely miscible mixtures
(ii) Validate the behavior of mixing properties with the literature
(iii) Represent and model the binary liquid-liquid equilibria, in order to obtain the behavior of the mixture
(iv) Represent and model the ternary liquid-liquid equilibria, in order to obtain the behavior of the mixture
(v) Find the optimal solvent for the separation whose main component is guaiacol

2. Hypothesis

Polar phenols form a single phase with polar molecules at ambient temperatures, so it is expected that, guaicol form a single phase at temperatures below 333 K with methanol, ethanol and acetone. On the other hand, it should forms a liquid-liquid equilibrium with hexadecane and dodecane, because they are apolar molecules. The behaviors can be modeled in a good way with PC-SAFT, COSMO RS and COSMO SAC.

2. BACKGROUND

1. Properties

1.1. Excess Volume

The excess molar volume is described as follows (Walas, 2013; Letcher, 1975)

$$V_m^E = V_{mix} - \sum x_i V_i^o \tag{2.1}$$

where x_i is the mole fraction of a component i, V_{mix} is the molar volume of the mixture and V_i^o is the volume of a component i. The excess volume may change due to various factors. The breakdowns of 1-1 and 2-2 intermolecular interaction which have a positive effect on the volume. The interaction is greater between 1-2 than 1-1 and 2-2 wich result a decrease of the volume. The difference in the size between 1 and 2 and the shape of the components that leads to a packing effect which may have positive or negative effect on the particular species involved. Finally, formation of new chemical species.

Changes on volume of binary mixing of liquids, V_m^E, at constant pressure and temperature is as an indicator of non-idealities in real mixtures (Renon & Prausnitz, 1968). In this work the excess molar volume will be measured by the indirect method. The details for the instrument used in this work are given in Section 2, a theoretical explanation of the technique is given here. The development of highly accurate vibrating tube densitometers has made it possible to determine, V_m^E with acceptable accuracy from the mixture density using the following equation:

$$V^{\mathrm{E}} = \frac{x_1 M_1 + x_2 M_2}{\rho} - \left(\frac{x_1 M_1}{\rho_1}\right) - \left(\frac{x_2 M_2}{\rho_2}\right) \tag{2.2}$$

where x_1 and x_2 are mole fractions, M_1 and M_2 are molar masses of the compounds, ρ_m is the density of the mixture and ρ_i represent the density to the component 1 or 2 respectively.

1.2. Liquid-liquid equilibria

When two phases are immiscible and there is transfer of substances from one phase to another, then phase separation is involved. There is exchange of constituents from each phase into the other when phases are brought into contact, this happens until the composition of each phase attains a constant value and this state of the phases is called macroscopic equilibrium. The phases in contact maybe vapour-liquid, liquid-liquid. The equilibrium composition of two phases are usually different from one another and this difference makes it possible to separate mixtures by distillation, extraction and other phase contacting processes.

The experimental study of the liquid-liquid phase balance of multi-component systems is of great importance in industrial phase extraction processes liquid, since it is required that the solvents chosen are not toxic to the process, more efficient, cheaper, more selective and less corrosive. For this reason, it is indispensable have reliable experimental data on liquid-liquid phase equilibrium of the compounds of interest.

In liquid liquid extraction two components in solution are separated by their distribution between the two immiscible phases with the addition of a third component. Solvent or the entrainer is the liquid added to the solution for the extraction process. This solvent takes up part of the components of the original solution and forms an immiscible layer with the remaining solution. Extract is the solvent layer and the other layer composed of the remaining original solution plus the solvent left is called the raffinate. Petroleum industry extensively uses the liquid liquid extraction process in separating hydrocarbons. The knowledge of liquid-liquid equilibrium (LLE) is necessary for design and optimization of a new separation process.

The requirement of thermodynamics for any type of phase equilibrium is that the compositions of each species in each phase in which it appears must meet the balance criteria (Sandler, 2017; Prausnitz, Lichtenthaler, & de Azevedo, 1998).

$$f^I(T, P, x^I) = f^{II}(T, P, x^{II}) \tag{2.3}$$

Entering the definition of the activity coefficient in the equation:

$$x_i^I \gamma_i^I(T, P, x^I) = x_i^{II} \gamma_i^{II}(T, P, X^I I) i = 1, 2, 3... \tag{2.4}$$

The compositions of the coexisting phases satisfy the equations:

$$\sum_{i=1}^{c} x_i^I = 1 \tag{2.5}$$

$$\sum_{i=1}^{c} x_i^{II} = 1 \tag{2.6}$$

Where f^I, f^{II} are the fugacities, x_i^I, x_i^{II} are the molar fractions and $\gamma_i^I, \gamma_i^{II}$ are the activity coefficients of component i in phase I and II respectively.

2. Thermodynamic Modeling

Systems of interest in this study are related to the separation of methoxyphenols from bio-oil with different solvents such as methanol, ethanol and acetone. Thus, guaiacol was used as model compound for the methoxyphenols meanwhile dodecane and hexadecane were used as alkanes model. Additionally, methanol, ethanol and acetone were used as solvents model. All calculation and analysis were performed using the Aspen Plus simulator (ASPEN Plus © v10 software). With the defined components of the system, three thermodynamics models were chosen to simulate the experimental data.

To evaluate the accuracies of the thermodynamic models generated in this work with regard to each density and equilibrium calculation, the root-mean-square deviation RMSD

$$\mathrm{RMSD} = \sqrt{\frac{\sum_{n=1}^{N} \left(\hat{y}_n - y_n\right)^2}{N}} \tag{2.7}$$

where N represents the total number of experimental samples used for regression and y denotes the property that the model.

2.1. PC-SAFT

The modeling of different thermodynamic properties such as density or phase equilibrium with an equation of state requires the calculation of the fugacity coefficients. PC-SAFT proposed by Gross and Sadowski in 2001 (Gross & Sadowski, 2001), uses Equation 2.8 to calculate the transience coefficients.

$$\ln \varphi_i = \frac{\mu_i^{res}}{RT} - \ln(Z) \tag{2.8}$$

where μ_i^{res} is the residual chemical potential and Z is the real gas coefficient. To calculate these factors, it is necessary to calculate the residual Helmholtz energy with the following expression:

$$\mathrm{a^{res}} = \mathrm{a^{hc}} + \mathrm{a^{disp}} + \mathrm{a^{assoc}} + \mathrm{a^{dipol}} \tag{2.9}$$

where $\mathrm{a^{hc}}$,$\mathrm{a^{disp}}$,$\mathrm{a^{assoc}}$,$\mathrm{a^{dipol}}$ account for the Helmholtz-energy contributions due to hard-chain repulsion, dispersion, association and dipole interactions. The objective of the thermodynamic modeling approach was target a precise description of the experimental data to allow subsequent process plant simulation of the process with PC-SAFT in ASPEN Plus. For dodecane and hexadecane association and dipole terms are not necessary meanwhile for alcohols the dipole term its set 0. The objective of the thermodynamic model is

Table 2.1. Pure-Component Parameters of the Perturbed-Chain SAFT Equation of State

Component	m	$\sigma(\dot{A})$	ϵ/κ (K)	$\kappa^{A_i B_i}$	$\epsilon^{A_i B_i}/\kappa$ (K)	μ	x_p
Guaiacol	2.8592	3.8352	346.17	0.0126454	1732.43	0	0
Dodecane	5.3060	3.8959	249.21	0	0	0	0
Hexadecane	6.6485	3.9552	254.70	0	0	0	0
Methanol	1.5255	3.2300	188.90	0.035176	2899.5	0	0
Ethanol	1.23058	4.1057	316.91	0.0033	2811.02	0	0
Acetone	2.1873	3.6028	245.49	0	0	2.72	0.297

to obtain an accurate description of the experimental data to allow the subsequent simulation with PC-SAFT. Pure chemical species parameters for dodecane, hexane, methanol, ethanol and acetone were taken from literature and were not regressed to experimental data. Parameters for guaiacol were regressed to experimental vapor pressure and liquid density data obtained from NIST interface in ASPEN Plus. Parameter regression for the PC-SAFT parameters was performed using ASPEN Plus © v10 software. Parameter regression was with the default algorithm options. Parameters used in this work are shown in Table 2.1, as they were set in the Aspen Plus simulator.

To describe mixtures of compounds, Berthelot-Lorenz mixing rules are used for interactions that occur between two components i and j as shown in Equation 1 and 2

$$\sigma_{\mathrm{ij}} = \frac{1}{2}\left(\sigma_{\mathrm{i}} + \sigma_{\mathrm{j}}\right) \tag{2.10}$$

$$\mathrm{u_{ij}} = \sqrt{\mathrm{u_i u_j}} \cdot \left(1 - \mathrm{k_{ij}}\right) \tag{2.11}$$

The binary interaction parameter k_{ij} is an adjustment parameter that describes deviations in the dispersion energy between the components. The parameter is fitted in Aspen Plus v10, to different experimental and literature data to obtain a better description of the interactions in the ternary mixture.

2.2. COSMO based model

COSMO based models calculations were carried out following procedure. Quantum chemical software Gaussian 0343 was used to optimize the molecular geometries of the guaiacol and generate the corresponding COSMO file. For dodecane, hexadecane, methanol, ethanol and acetone the COSMO file avaiable in Cosmologic database was used. COSMO files were used as an input in COSMOthermX (version C3.0 Release 18.0)(Eckert & Klamt, 2010) software, and its implicit parametrization (BP TZVP 18) was used to obtain the σ-profiles and σ-potentials of the compounds. For compounds with more than one conformation available, all were considered for calculations. Then, the σ-profile that contains the main chemical information necessary to predict interactions(Palomar, Gonzalez-Miquel, Bedia, Rodriguez, & Rodriguez, 2011), were introduced to the ASPEN Plus software where COSMO-RS and COSMO-SAC models are available to predict the liquid-liquid equilibrium.

Thermodynamic properties of the mixture, such as activity coefficients and liquid-liquid equilibrium can be derived from the chemical potentials. This properties have been calculated with the Equation 2.12

$$x_i^{\mathrm{I}}\gamma_i^{\mathrm{I}} = x_i^{\Pi}\gamma_i^{\mathrm{I}} \tag{2.12}$$

where indices I and II denote the two liquid phases, γ_i are the activity coefficients computed by COSMO and x_i are the mole fractions. LLE binary mixtures were calculated at 313.15 K: guaiacol + methanol, guaiacol + hexadecane, methanol + dodecane, methanol + hexadecane at differents temperatures and the ternary systems of guaiacol + dodecane + methanol, guaiacol + hexadecane + methanol, guaiacol + dodecane + ethanol, guaiacol + hexadecane + ethanol, guaiacol + dodecane + acetone, guaiacol + hexadecane + acetone.

3. METHODOLOGY

1. Chemicals

All the compounds used in the study are shown in Table 3.1 with their respective purities and source. All of them were used from the same batch. The mixtures used in this work were prepared gravimetrically using an analytic balance (Sartorius Practum 224-1s, Germany) with a repeatability of 0.1 mg.

Table 3.1. Specifications of chemicals used in this work as molar mass (M), CAS number, supplier and purity

Fluid	M (g·mol^{-1})	CAS number	Supplier	Type	Purity (wt%)
guaiacol	124.14	90-05-1	Sigma-Aldrich	For Synthesis	≥99.0
dodecane	170.34	112-40-3	Merck	For Synthesis	≥99.0
hexadecane	226.45	544-76-3	Merck	For Synthesis	≥99.0
methanol	32.04	67-56-1	Acros Organics	AcroSeal Extra dry	≥99.9
ethanol	46.07	64-17-5	Acros Organics	AcroSeal Extra dry	≥99.5
acetone	58.08	67-64-1	Merck	SupraSolv	≥99.0

2. Density and dynamic viscosity measurement

Different mixing compositions were prepared in a closed vial. Density was measured in a Anton Paar 4500 DMA Densimeter (Graz, Austria). It uses the Anton Paar's vibrating U-tube technology to provide density measuraments with an accuracy of 0.005 $kg \cdot m^{-3}$. The internal temperature is measured with an accuracy of 0.01 K using an integrated Pt 100 thermometers. The vibrating U-tube technology determines the density of a sample by

$$\rho = \frac{c}{4\phi^2 V} \cdot P^2 - \frac{M}{V} \tag{3.1}$$

where ρ is density, c is the spring constant, V is volume of the U-tube, P is oscillation period, and M is mass. The oscillation period, P, is known from the continuous oscillation

at a frequency, f, dependent on the density of the sample. This equation can be reduced to

$$\rho = A \cdot P^2 - B \tag{3.2}$$

where A and B are constants determined. The constants are determined using two known standards, air and water. The apparatus was calibrated with double distilled deionized, and degassed water, and dry air at atmospheric pressure. The viscosity was measured with a modular microviscometer Lovis 2000 ME provided by Anton Paar is used in conjunction with the DMA 4500 to perform dynamic viscosity measurements. The measurements of viscosity with Lovis 2000 ME is based on the falling ball principle. The microviscometer is equipped with three calibrated glass capillaries of different diameter, in addition to steel balls. The time taken by the steel ball to fall from one side of the capillary to the other of the sample filled capillary at a certain angle is measured. The time and the density were used to calculate the dynamic viscosity by

$$\eta = k_1 \cdot (\rho_b - \rho_s) \cdot t_1 \tag{3.3}$$

where η is the dynamic viscosity, k_1 a calibration constant, ρ_b the steel ball density, ρ_s the density of the measured sample in the DMA 4500 and t_1 the ball rolling time. The calibration of the capillaries was done by the manufacturer using fluids with standard viscosity and measured in our laboratory using the same standards and different solvents as methanol, water and glycerol. Viscosity measurements was given with a repeatability of 0.1%, the measurement accuracy varies between 0.17% and 0.50% depending on the size of the capillary and the temperature.

3. Liquid-liquid measurement

The chemicals used in this equilibrium were dodecane, hexadecane, guaiacol, methanol, ethanol and acetone. The two organics compounds form a liquid-liquid equilibrium with the guaiacol at the measured temperatures. The binary mixture was introduced into a cell

in known proportions. The cell temperature was controlled with a thermostatic bath and a thermometer with a repeatability of 0.1 K were used to monitor the temperature of the cell. The mixture was vigorously stirred with a magnetic stirrer for 4 h and let stand for 4 h to obtain two clear and transparent phases woth a well-defined interface. The samples were dissolved in chloroform, before being analyzed by the GC. The same procedure was performed for mixing polar and arganic compounds. The samples were analyzed with a gas chromatograph (Nexis GC-2030 - Shimadzu) equipped with a flame ionization detector, split-splitless injector and a Elite-1 100 non-polar capillary column (30 m $\times$ 0.53 mm $\times$ 3.0 μm) with nitrogen as carrier gas flow rate of 15 $cm^3 \cdot min^{-1}$. Temperature program included isothermal analysis at 37 ^{o}C, which lasted 3 min. Then a ramp of 10 ^{o}C$\cdot$ min^{-1} was used to increase temperature to 250 ^{o}C. The external standard method was used to quantify the amount of each compounds in the systems. The analysis was performed at least three times for each sample. A series of LLE data was obtained by changing the feed composition. In this study, all measurements were performed in triplicate to decrease the standard deviation.

4. RESULTS AND DISCUSSION

1. Pure compounds

Table 4.1 shows the density and dynamic viscosity measurements of pure compounds at temperatures between 293.15 K and 333.15 K, at atmospheric pressure.

Table 4.1. Densities ($g \cdot cm^{-3}$) and viscosities (mPa·s) of guaiacol, dodecane, hexadecane, methanol, ethanol and acetone at different temperatures (K) and a pressure of 101.3 kPa.

	293.15 K	303.15 K	313.15 K	323.15 K	333.15 K
	Density ($g \cdot cm^{-3}$)				
guaiacol	1.13304	1.12342	1.11370	1.10392	1.09410
dodecane	0.74879	0.74158	0.73430	0.72699	0.71965
hexadecane	0.77342	0.76652	0.75962	0.75271	0.74579
methanol	0.79130	0.78191	0.77238	0.76272	0.75288
ethanol	0.78936	0.78080	0.77297	0.76316	0.0.75401
acetone	0.79000	0.77853	0.76687	0.75497	-
	Viscosity (mPa·s)				
guaiacol	6.803	4.505	3.215	2.424	1.904
dodecane	1.487	1.246	1.062	0.919	0.806
hexadecane	3.419	2.709	2.202	1.828	1.544
methanol	0.586	0.511	0.450	0.400	0.357
ethanol	1.195	0.991	0.828	0.699	0.593
acetone	0.336	0.310	0.288	0.269	-

The results obtained in this work for density and viscosity are consistent with the literature review. Also, for all systems, as expected, there is a tendency to decrease density with increasing temperature. In addition, it is shown that the error is quite low with respect to the literature, so it can be assumed again that the measurements are consistent.

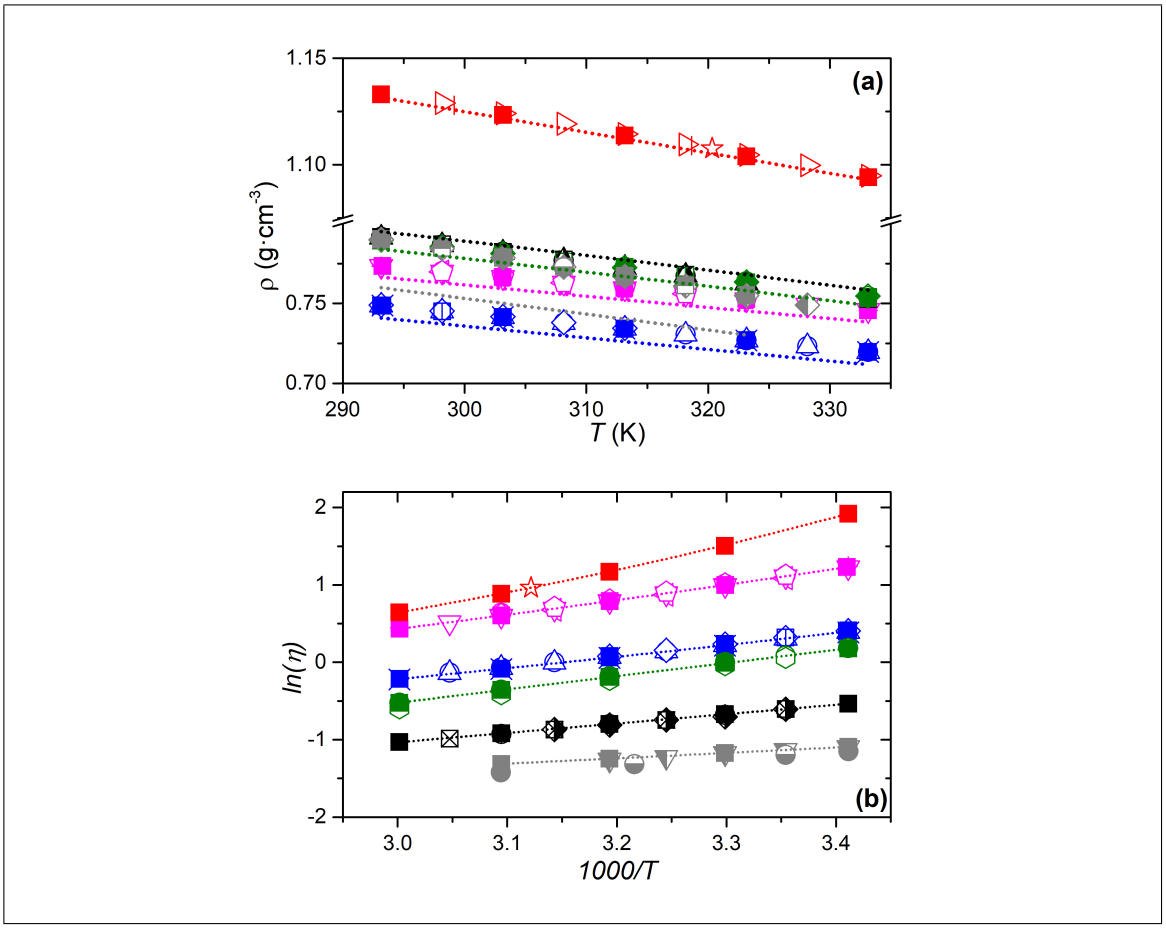

Figure 4.1. **(a)** Density (g·cm^{-3}) **(b)** logarithm of dynamic viscosity as a function of 1000 times the inverse temperature of guaiacol (■), dodecane (■), hexadecane (■), methanol (■), ethanol (■) and acetone (■) as a function of temperature at a pressure of 101.3 kPa. Dotted line (···) represents in (a) PC-SAFT model and in (b) VFT model.

Figure 4.1 (a) shown the density experimental data of pure solvents, PC-SAFT model and the comparison with the collected literature data. The root mean square deviation of the model are presented in table 4.4 where all errors are less than 2.5%. Viscosity is compared with literature and VFT model are shown graphically en Figure 4.1 (b). As expected, the viscosity decreases with temperature, hence, the property is correlated as an exponential decreasing function of temperature. A higher viscosity is related to stronger molecular interactions and a low steric impediment, while the temperature increases the

interactions decrease, consequently the viscosity also does. On the other hand, if the temperature decreased, molecular interactions became relevant and the viscosity increases. As in the case of density, the compound with the highest viscosity is guaiacol, since it has polar interactions. Viscosity data were fitted to the Vogel-Fulcher-Tamman (VFT, with fitting parameters A, B and T_0) shown in Equation 4.1.

$$\eta_{VFT}(T) = A \exp\left(\frac{B}{T - T_0}\right) \tag{4.1}$$

The root mean square deviation of the model are presented in table 4.2 where all errors are less than 4% therefore it is an acceptable modeling.

2. Excess volume and mixture viscosity

Guaiacol as state above, is completely miscible with methanol, ethanol and acetone. Mixture density and viscosity data are shown in Table 4.3 and 4.5, respectively. The excess volume (V^E) calculated using Equation 2.2, explain the molecular interactions, non-idealities and molecular arrangement of the mixrture.

Figure 4.2 (a) shows the excess volume of the binary mixture of guaiacol + methanol and Figure 4.2 (b) guaiacol + ethanol and Figure 4.2 (c) guaiacol + acetone as a function of the mole fraction of guaiacol, along with PC-SAFT model fitting. Negative excess volume 1-2 interactions have to be stronger than 1-1/2-2 interactions to provide phase separation (Amore, Horbach, & Egry, 2011).

The density model is better than the excess volume model, because the PC-SAFT parameters are with the density data. Also, the excess volume is more sensitive to small variations.

Table 4.2. Viscosity fitting coefficients from VFT equation 4.1 of pure compounds used in this work and the respective root mean square deviation (%RMSD) of the correlation

	A	B	T_0	RMSD
guaiacol	0.1017	387.2103	201.0302	0.0021
dodecane	0.0503	613.6352	112.004	0.001
hexadecane	0.056	686.1781	126.2325	0.0019
methanol	0.0099	1176.2032	4.7478	0.0014
ethanol	0.0014	2339.9988	-53.3301	0.0031
acetone	0.0423	517.8163	43.1726	0.0001

Figure 4.3 shows experimental data of the viscosities of mixtures composed by (a) guaiacol + methanol, (b) guaiacol + ethanol and (c) guaiacol + acetone as a function of the guaiacol molar fraction at different temperatures. In general the viscosity decreases as the temperature increases. This is explained because it increases the kinetic energy of the particles, doing less resistance to movement. In addition, it can be seen that the viscosity increases as the molar fraction of guaiacol increases. This is explained because guaiacol has a higher viscosity than the other compounds. In this case, the systems is not modeled because the important is the behavior of the mixture and is not necessary a thermodynamic model.

3. Binary liquid-liquid equilibria

The LLE experimental results over a wide composition range as well as PC-SAFT, COSMO-SAC and COSMO-RS model fitting are illustrated in Figure 4.4. It is shown the guaicol forms a liquid-liquid equilibria with the dodecane and hexadecane. In the case of hexadecane it is shown that the behavior is in accordance with the literature. Table 4.7 list the compositions of two liquid phases. As shown in the Figure 4.4, PC-SAFT model is the best to explain the behavior, it is because it has an adjusted binary parameter, shown in Table 4.6. If the pair of compounds has only one component of the binary interaction parameter, it does not depend on the temperature. If it has two components, the binary interaction parameter depends on the temperature. The liquid-liquid use the

Table 4.3. Densities ($g \cdot cm^{-3}$) and excess volume ($cm^3 \cdot mol^{-1}$) of guaiacol + solvents liquid mixture at different temperatures (K), compositions of guaiacol (x_1) and a pressure of 101.3 kPa.

guaiacol(1) + methanol(4)										
	Density ($g \cdot cm^{-3}$)					Excess molar volume ($cm^3 \cdot mol^{-1}$)				
x_1	293.15 K	303.15 K	313.15 K	323.15 K	333.15 K	293.15 K	303.15 K	313.15 K	323.15 K	333.15 K
0.1203	0.8970	0.8876	0.8781	0.8684	0.8585	-0.7284	-0.7618	-0.7943	-0.8261	-0.8574
0.2335	0.9647	0.9553	0.9454	0.9358	0.9249	-1.1127	-1.1587	-1.1835	-1.2355	-1.2210
0.3595	1.0182	1.0086	0.9987	0.9887	0.9786	-1.3372	-1.3744	-1.4089	-1.4403	-1.4697
0.4745	1.0535	1.0437	1.0338	1.0237	1.0135	-1.3682	-1.3975	-1.4228	-1.4448	-1.4644
0.6010	1.0821	1.0723	1.0623	1.0522	1.0419	-1.2385	-1.2572	-1.2726	-1.2846	-1.2945
0.7218	1.1025	1.0927	1.0827	1.0727	1.0625	-0.9866	-0.9974	-1.0046	-1.0094	-1.0123
0.8396	1.1177	1.1079	1.0980	1.0881	1.0780	-0.6316	-0.6361	-0.6377	-0.6367	-0.6368
0.9363	1.1276	1.1179	1.1081	1.0982	1.0883	-0.2693	-0.2712	-0.2707	-0.2685	-0.2678
guaiacol(1) + ethanol(5)										
	Density ($g \cdot cm^{-3}$)					Excess molar volume ($cm^3 \cdot mol^{-1}$)				
x_1	293.15 K	303.15 K	313.15 K	323.15 K	333.15 K	293.15 K	303.15 K	313.15 K	323.15 K	333.15 K
0.1204	0.8703	0.8613	0.8521	0.8427	0.8331	-0.7887	-0.8001	-0.7475	-0.8140	-0.8191
0.2398	0.9336	0.9243	0.9147	0.9049	0.8949	-1.2431	-1.2514	-1.2031	-1.2573	-1.2571
0.3598	0.9843	0.9746	0.9648	0.9548	0.9445	-1.4410	-1.4429	-1.3952	-1.4332	-1.4260
0.4808	1.0252	1.0154	1.0053	0.9952	0.9849	-1.4268	-1.4215	-1.3753	-1.3984	-1.3850
0.6008	1.0585	1.0486	1.0386	1.0284	1.0181	-1.2870	-1.2779	-1.2377	-1.2509	-1.2357
0.7199	1.0871	1.0771	1.0671	1.0570	1.0468	-1.1378	-1.1282	-1.0982	-1.1063	-1.0941
0.8394	1.1083	1.0985	1.0885	1.0785	1.0685	-0.6370	-0.6314	-0.6100	-0.6095	-0.5999
0.9612	1.1276	1.1179	1.1081	1.0983	1.0884	-0.1656	-0.1630	-0.1570	-0.1556	-0.1531
guaiacol(1) + acetone(6)										
	Density ($g \cdot cm^{-3}$)					Excess molar volume ($cm^3 \cdot mol^{-1}$)				
x_1	293.15 K	303.15 K	313.15 K	323.15 K	333.15 K	293.15 K	303.15 K	313.15 K	323.15 K	333.15 K
0.1204	0.8703	0.8613	0.8521	0.8427	0.8331	-0.7887	-0.8001	-0.7475	-0.8140	-0.8191
0.2398	0.9336	0.9243	0.9147	0.9049	0.8949	-1.2431	-1.2514	-1.2031	-1.2573	-1.2571
0.3598	0.9843	0.9746	0.9648	0.9548	0.9445	-1.4410	-1.4429	-1.3952	-1.4332	-1.4260
0.4808	1.0252	1.0154	1.0053	0.9952	0.9849	-1.4268	-1.4215	-1.3753	-1.3984	-1.3850
0.6008	1.0585	1.0486	1.0386	1.0284	1.0181	-1.2870	-1.2779	-1.2377	-1.2509	-1.2357
0.7199	1.0871	1.0771	1.0671	1.0570	1.0468	-1.1378	-1.1282	-1.0982	-1.1063	-1.0941
0.8394	1.1083	1.0985	1.0885	1.0785	1.0685	-0.6370	-0.6314	-0.6100	-0.6095	-0.5999
0.9612	1.1276	1.1179	1.1081	1.0983	1.0884	-0.1656	-0.1630	-0.1570	-0.1556	-0.1531

Standard uncertainties u are $u(x_1)$=0.005, $u(T)$=0.01 K, $u(P)$= 1 kPa. amd $u(\rho)$=0.0004 $g \cdot cm^{-3}$

dependent temperature parameter because is sensible to a small variations. For the cases of dodecane/ethanol and hexadecane/ethanol the binary interaction parameter was not used, because was not possible to fit one to explain the behavior better than with out it. The binary interaction parameter shown in Equation 4.2.

$$k_{ij} = a_{ij} + b_{ij}/T \tag{4.2}$$

Table 4.4. Root mean square deviation of pure and mixture systems

RMSD	
Pure density	
	PC-SAFT
guaicol	0.0014
dodecane	0.0080
hexadecane	0.0072
methanol	0.0048
ethanol	0.0054
acetone	0.0247
Mixture density	
	PC-SAFT
guaiacol+methanol	0.0063
guaiacol+ethanol	0.0081
guaiacol+acetone	0.1140

COSMO-SAC and COSMO-RS only uses the shape of the molecule, are predictive models and both has the same base. The difference between COSMO-RS and COSMO-SAC is that RS has more than 30 reimplementations and COSMO-SAC is one of this reimplementations. Although they slightly differ with respect to the parameterization and the details of the implementation, most of them are name as COSMO-RS in the literature. The values of root-mean-square-deviation for the binary systems are presented in table 4.8. PC-SAFT model present the lower deviated values from the experimental data. In the other hand, COSMO-SAC present the higher deviation. This can be explained because PC-SAFT conforms to molecular interactions and can better predict the aliphatic phase, while COSMO predicts behavior based on the shape of the molecule and does not predict the aliphatic phase. As stated earlier, COSMO-RS presents better modeling, since it has several improvements since its creation.

Table 4.5. Viscosities (mPa·s) of guaiacol + solvent liquid mixture at different temperatures (K), compositions of guiacol (x_1) and a pressure of 101.3 kPa.

guiacol(1) + methanol(4)					
	Viscosity (mPa·s)				
x_1	293.15 K	303.15 K	313.15 K	323.15 K	333.15 K
0.121	1.097	0.911	0.768	0.654	0.562
0.233	1.450	1.172	0.961	0.803	0.680
0.360	2.894	2.147	1.649	1.308	1.063
0.475	4.044	2.865	2.134	1.647	1.316
0.601	5.120	3.479	2.514	1.906	1.498
0.722	5.860	3.898	2.850	2.139	1.667
0.840	6.580	4.321	3.059	2.291	1.790
0.935	6.866	4.517	3.201	2.396	1.877
guiacol(1) + ethanol(5)					
	Viscosity (mPa·s)				
x_1	293.15 K	303.15 K	313.15 K	323.15 K	333.15 K
0.120	1.713	1.368	1.108	0.912	0.759
0.240	2.410	1.839	1.440	1.156	0.944
0.360	3.242	2.374	1.803	1.413	1.135
0.481	4.158	2.938	2.175	1.673	1.327
0.601	5.036	3.445	2.502	1.896	1.491
0.720	5.730	3.840	2.753	2.074	1.626
0.839	6.292	4.177	2.975	2.238	1.752
0.961	6.701	4.432	3.154	2.376	1.863
guaiacol(1) + acetone(6)					
	Viscosity (mPa·s)				
x_1	293.15 K	303.15 K	313.15 K	323.15 K	333.15 K
0.1266	2.008	1.681	1.428	1.230	1.072
0.2355	1.742	1.469	1.258	1.091	0.956
0.3387	1.523	1.314	1.128	0.986	0.871
0.4335	1.413	1.203	1.041	0.920	0.807
0.5749	1.264	1.083	0.941	0.829	0.737
0.6688	1.200	1.029	0.898	0.793	0.707
0.7740	1.131	0.973	0.850	0.752	0.671
0.8931	1.088	0.937	0.818	0.724	0.646

Standard uncertainties u are $u(x_1)$=0.005, $u(T)$=0.01 K, $u(P)$= 1 kPa. Relative standard uncertainties $u_r(\eta)$=0.06

4. Ternary liquid-liquid equilibria

Liquid-liquid separation is one of the most popular process in industry to extract aromatics from aliphatics. The selection of the appropriate solvent is of great importance to ensure the success of the liquid-liquid extraction. The best solvents have good selectivity and capacity, high thermal stability, good availability, low cost, high surface tension and

Table 4.6. PC-SAFT binary interaction parameters k_{ij} for liquid-liquid equilibrium

	a_{ij}	b_{ij} [1/K]	type of data used for fitting	temperature range (K)	RMSD (%)
Guaiacol/dodecane	-0.01559	9.45499	liquid-Liquid (own data)	293.15-333.15	3.22
Guaiacol/hexadecane	-0.00545	5.756795	liquid-Liquid (own data)	293.15-338.15	2.33
Guaiacol/methanol	-0,02088	0	vapor-Liquid	337.8-477.9	9.90
Guaiacol/ethanol	-0,01831	0	vapor-Liquid	290	0.28
Guaiacol/acetone	-0,10025	0	vapor-Liquid	329.05-457.55	1.22
Dodecane/methanol	0.09652	-16.69971	liquid-Liquid (own data)	293.15-333.15	1.77
Dodecane/ethanol	0	0			
Dodecane/acetone	-0,00858	0	vapor-Liquid	333.15	0.08
Hexadecane/methanol	0.07242	-8.51037	liquid-Liquid (own data)	293.15-333.15	0.73
Hexadecane/ethanol	0	0			
Hexadecane/acetone	-0,00033	0	vapor-Liquid	333.15	0.06

low to moderate viscosity (Müller, Berger, Blass, Sluyts, & Pfennig, 2000). Cheaper and environmentally friendly solvents is another feature to consider."Green" solvents have a low toxicity, persistence and volatility (Kislik, 2012). All the ternary systems are new and there is not comparison with the literature. Figure 4.5 shows the tine lines in the systems guaiacol + aliphatics + solvents. The best analysis is provided by calculating the capacity and selectivity of the solvent at different compositions of the two phases. The capacity of the solvent to dissolve dodecane or hexadecane is defined as the distribution ratio, D_i. It can be defined in mass fraction ($D_{i,w}$) in eq 4.3. Where $w_i^{\alpha or \beta}$ is the mass fraction of compound i in the α or β phase, calling α as the guaiacol rich phase and β as the aliphatic rich phase.

$$D_{w,i} = \frac{w_i^a}{w_i^\beta} \tag{4.3}$$

A good solvent has to shown a lower distribution ratio for the aliphatic than the aromatic. A high distribution ratio of the aromatics allows the use of less solvent in the liquid-liquid extraction. The selectivity is calculated as the distribution ratio of the aromatic divided by the distribution ratio of the aliphatic in mass fraction.

Table 4.7. Experimental liquid-liquid equilibrium data, in weight fraction, for the binary system at atmospheric pressure

guaiacol(1) + dodecane(2)				
	alkane rich phase		guaiacol rich phase	
T (K)	w_1	w_2	w_1	w_2
293.15	0.1089	0.8911	0.9467	0.0533
303.15	0.1441	0.8559	0.93	0.07
313.15	0.203	0.797	0.9156	0.0844
323.15	0.2931	0.7069	0.889	0.111
328.15	0.4081	0.5919	0.8546	0.1454
guaiacol(1) + hexadecane(3)				
	alkane rich phase		guaiacol rich phase	
T (K)	w_1	w_3	w_1	w_3
293.15	0.0689	0.9311	0.9684	0.0316
303.15	0.0941	0.9059	0.955	0.045
313.15	0.1318	0.8682	0.9395	0.0605
323.15	0.179	0.821	0.9142	0.0858
333.15	0.2462	0.7538	0.9011	0.0989
338.15	0.3003	0.6997	0.8956	0.1044
dodecane(2) + methanol (4)				
	alkane rich phase		guaiacol rich phase	
T (K)	w_2	w_4	w_2	w_4
293.15	0.9881	0.0118	0.0686	0.9313
303.15	0.9859	0.0140	0.0832	0.9168
313.15	0.9825	0.0175	0.0515	0.9486
323.15	0.9856	0.0144	0.1153	0.8847
333.15	0.9706	0.0294	0.1478	0.8522
hexadecane(3) + methanol (4)				
	alkane rich phase		guaiacol rich phase	
T (K)	w_3	w_4	w_3	w_4
293.15	0.9942	0.0.0058	0.0303	0.9697
303.15	0.9925	0.0075	0.0377	0.9623
313.15	0.9941	0.0059	0.0235	0.9765
323.15	0.9899	0.0101	0.0552	0.9448
333.15	0.9838	0.0162	0.0758	0.9242

$$S = \frac{D_{\text{aromatic}}}{D_{\text{diphatic}}} = \frac{w^{a}_{\text{aromatic}} / w^{\beta}_{\text{aromatic}}}{w^{a}_{\text{aliphatic}} / w^{\beta}_{\text{alphatic}}} \tag{4.4}$$

A hight selectivity is the consequence of a high distribution factor for the aromatic and low distribution factor for the aliphatic. Figure 4.6 shows the selectivity and distribution ratio for the guaicol + dodecane + methanol system at 313.15 K and Figure 4.7 shows the differents selectivities for solvent. In general, it is shown that as the concentration of guaiacol increases the selectivity decreases. Mixtures with methanol present the highest selectivities. This can be explained because methanol, is a small and polar molecule and is able to interact better with guaicol. High concentrations of guaiacol leads to lower selectivities, this is because by increasing the concentration of guaicol the interactions with the phenolic phase increase. Also, methanol has a strong H-bond aceptor zone wich make a strong interaction with the guaiacol. Figure 4.8 shows the different sigma profile and sigma potencial. Guaicol present a big apolar region and small H-bond donor section, methanol and ethanol have almost the same behavior, but methanol have a higher H-bond aceptor wich allows to interact better with the guaiacol. Best interactions are those that behave in the most similar way in the sigma potential, thus methanol is the best solvent to extract the guaciacol.

The behavior of the LLE of guaicol + aliphatic + solvets systems have been predicted with PC-SAFT, COSMO-RS and COSMO-SAC models. The root-mean-square-deviation between experimental and predicted values was determined to evaluate the performance of the models fitting LLE.The best model to represent the experimental data is PC-SAFT, present the lowest values of MRSD. PC-SAFT uses the binary systems to predict the ternary systems and COSMO is completely predictive, thus PC-SAFT is better than COSMO in the ternary equilibrium. As Figure 4.5 shows, the three models are able to predict equilibrium behavior. The values of root-mean-square-deviation for the ternary systems are presented in table 4.8.

Table 4.8. Root mean square deviation of binary and ternary systems

RMSD			
Binary LLE			
	PC-SAFT	COSMO-SAC	COSMO-RS
guaiacol+dodecane	0.0332	0.1842	0.1621
guaiacol+hexadecane	0.0233	0.1381	0.1136
dodecane+methanol	0.0177	0.0577	0.044
hexadecne+methanol	0.0078	0.0532	0.0416
Ternary LLE			
	PC-SAFT	COSMO-SAC	COSMO-RS
guaiacol+dodecane+methanol	0.0243	0.0624	0.0540
guaiacol+hexadecane+methanol	0.0184	0.0431	0.0368
guaiacol+dodecane+ethanol	0.0431	0.0884	0.1144
guaiacol+hexadecane+ethanol	0.0381	0.0739	0.0656
guaiacol+dodecane+acetone	0.0939	0.1613	0.2165
guaiacol+hexadecane+acetone	0.0938	0.0995	0.1794

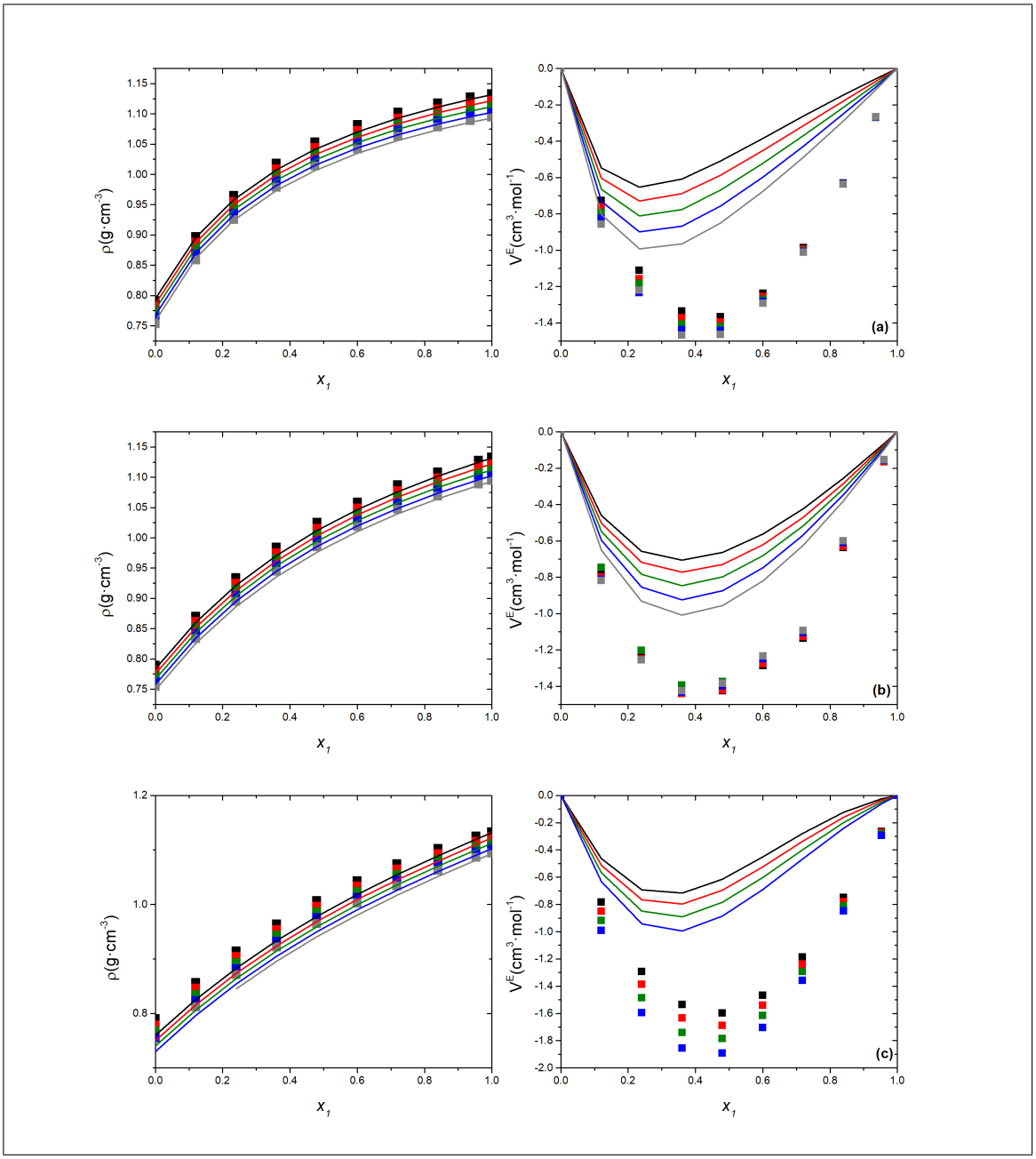

Figure 4.2. Density (g·cm^{-3}) and excess molar volume (cm^3·mol^{-1}) in terms of the mole fraction of guaiacol for the binary mixtures of **(a)** guiacol + methanol, **(b)** guaiacol + ethanol and **(c)** guiacol + acetone at a pressure of 101.3 kPa and different temperatures: 293.15 K (■), 303.15 K (■), 313.15 K (■), 323.15 K (■), and 333.15 K (■). The continuous line (–) represents the PC-SAFT model with parameters reported in Table 2.1 and 4.6.

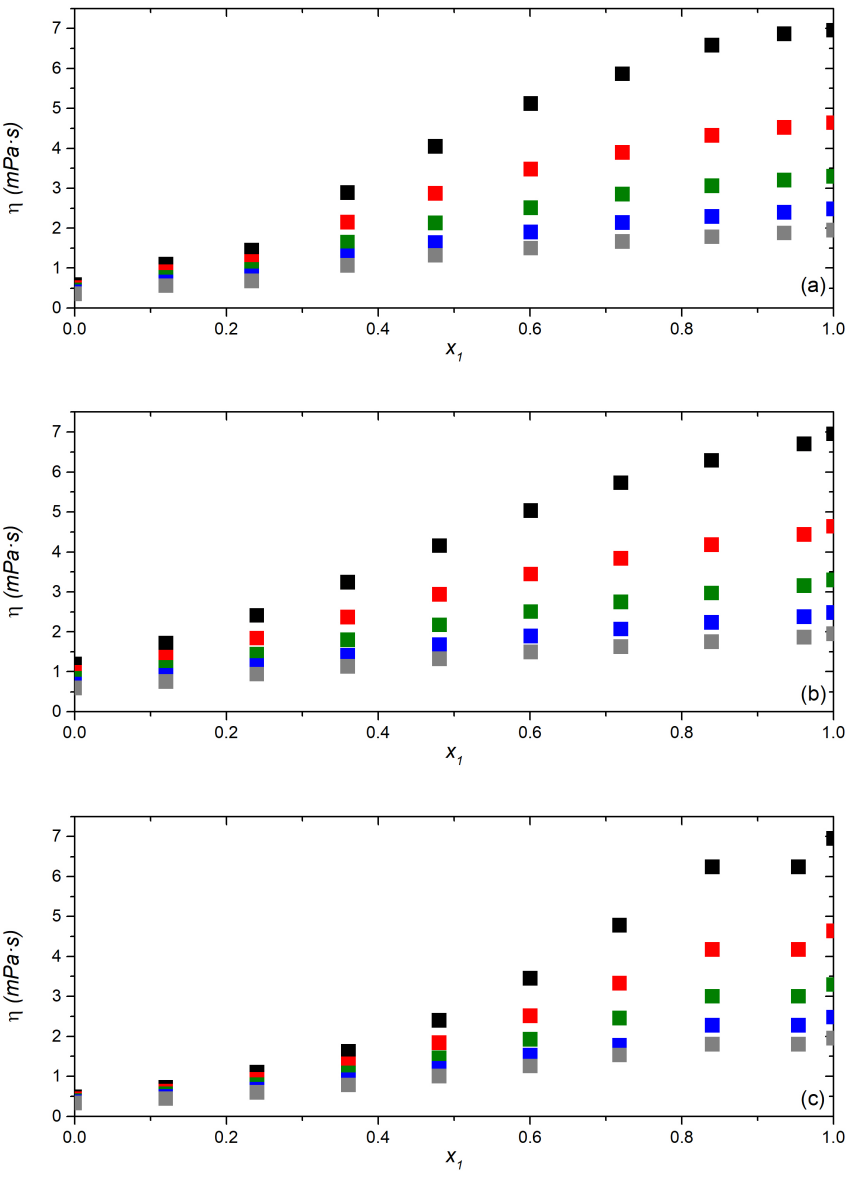

Figure 4.3. Dynamic viscosity (mPa·s) in terms of the mole fraction of guaiacol for the binary mixtures of **(a)** guaiacol + methanol and **(b)** guaiacol + ethanol and **(c)** guaiacol + acetone at a pressure of 101.3 kPa and different temperatures: 293.15 K (■), 303.15 K (■), 313.15 K (■), 323.15 K (■) and 333.15 K (■).

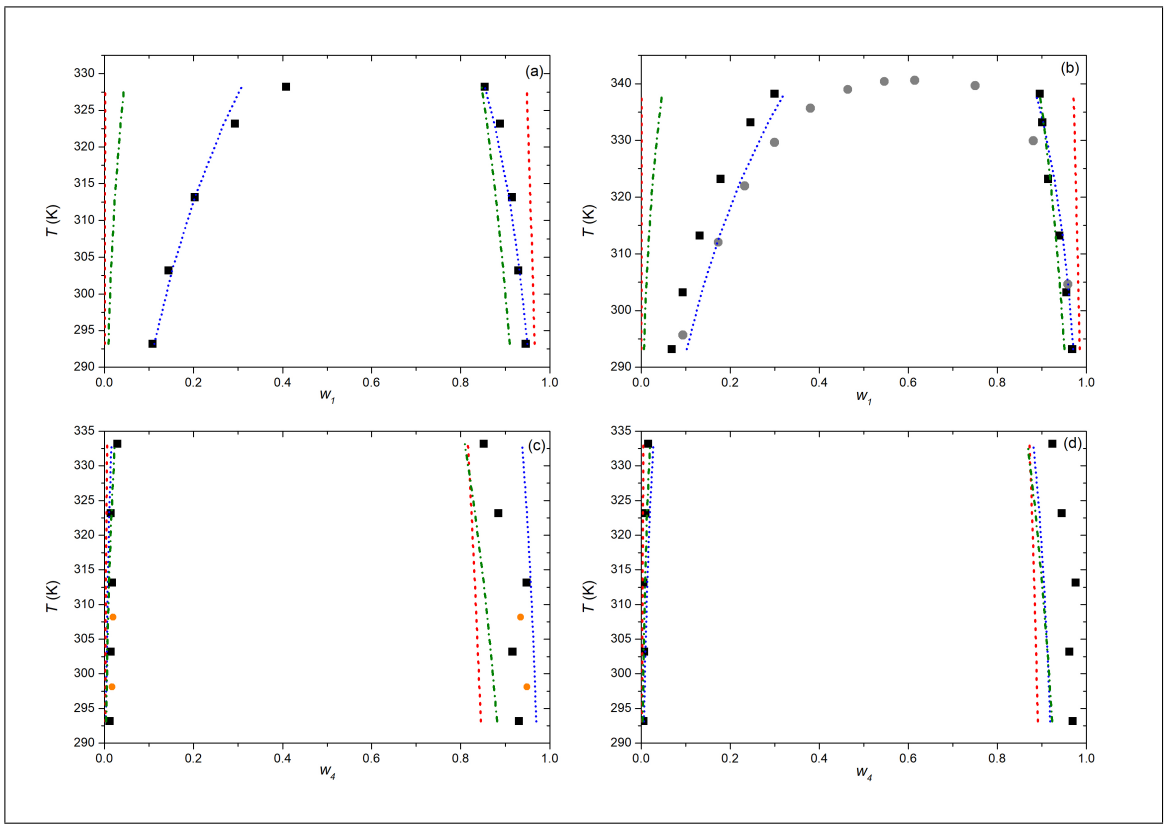

Figure 4.4. Liquid-liquid phase equilibria diagram of binary systems of **(a)** guaiacol(1) + dodecane, **(b)** guaiacol(1) + hexadecane, **(c)** methanol(4) + dodecane and **(d)** methanol(4) + hexadecane. Comparison with reported data (Ksiaczak & Kosiński, 1990) (●) and with (Casás et al., 2002)(●). The blue dotted line (···) represents represents the PC-SAFT, red dash line (- -) represent COSMO SAC and green dash doted line (- · -) represent COSMO RS model.

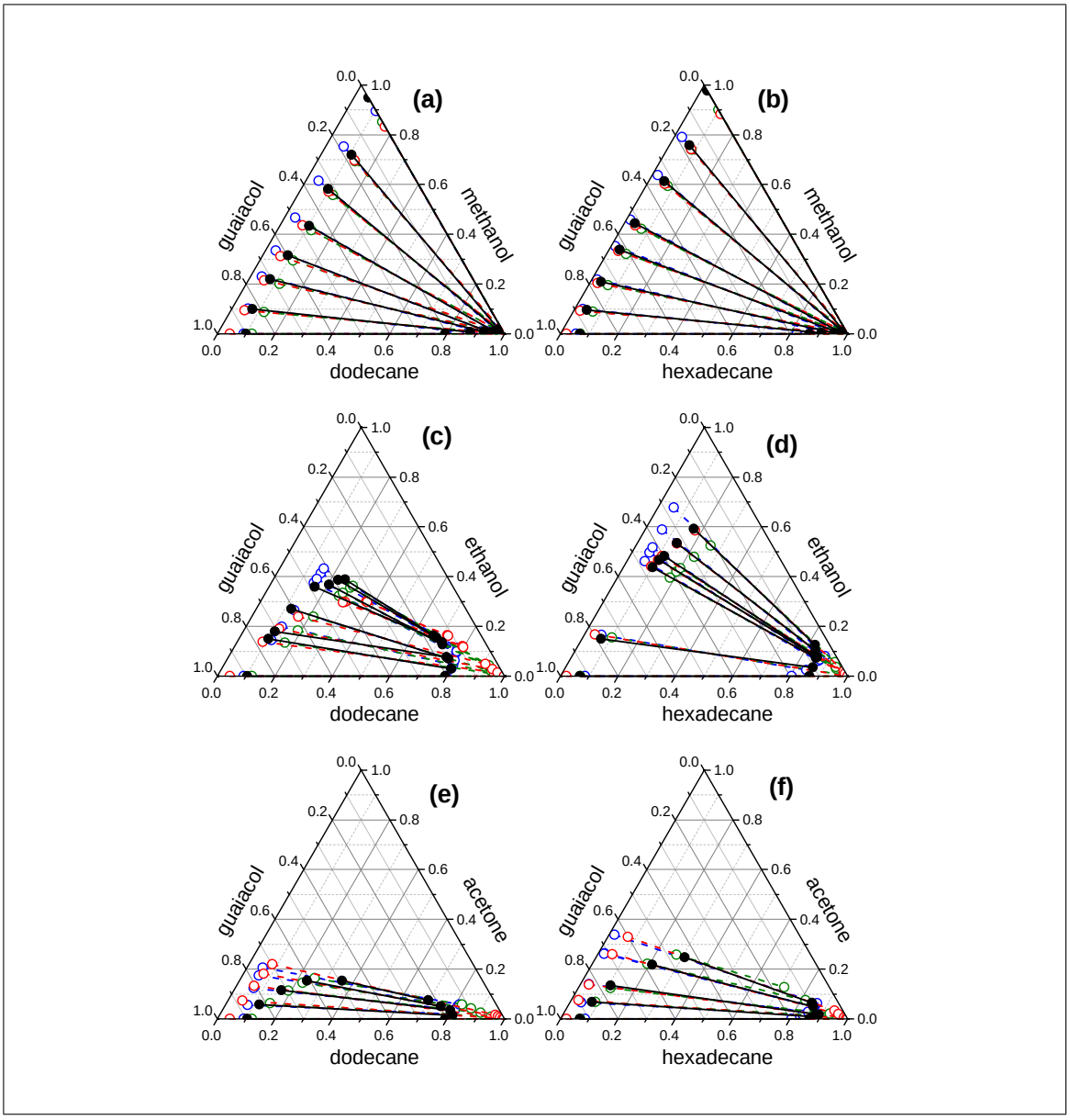

Figure 4.5. Liquid-liquid equilibrium of the ternary mixture of **(a)** guaiacol + dodecane + methanol, **(b)** guaiacol + hexadecane + methanol, **(c)** guaiacol + dodecane + ethanol, **(d)** guaiacol + hexadecane + ethanol, **(e)** guaiacol + dodecane + acetone, **(f)** guaiacol + hexadecane + acetone at 313.15 K in mass fraction. Experimental data (●), PC-SAFT (○), COSMO-RS (○) and COSMO-SAC(○)

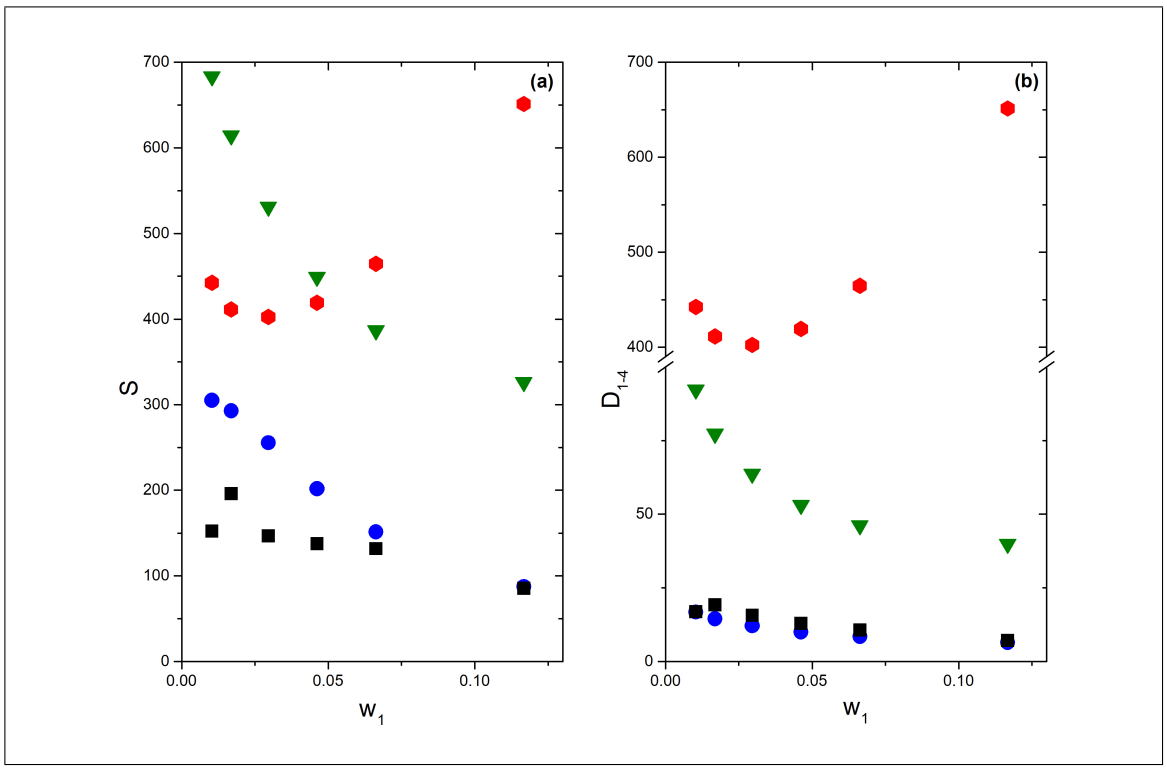

Figure 4.6. Selectivity **(a)** and distribution ratio **(b)** of guaiacol+dodecane+methano guaiacol + dodecane + methanol at 313.15 K in mass fraction. Experimental data (■), PC-SAFT (●), COSMO-RS (▼) and COSMO-SAC(⬢)

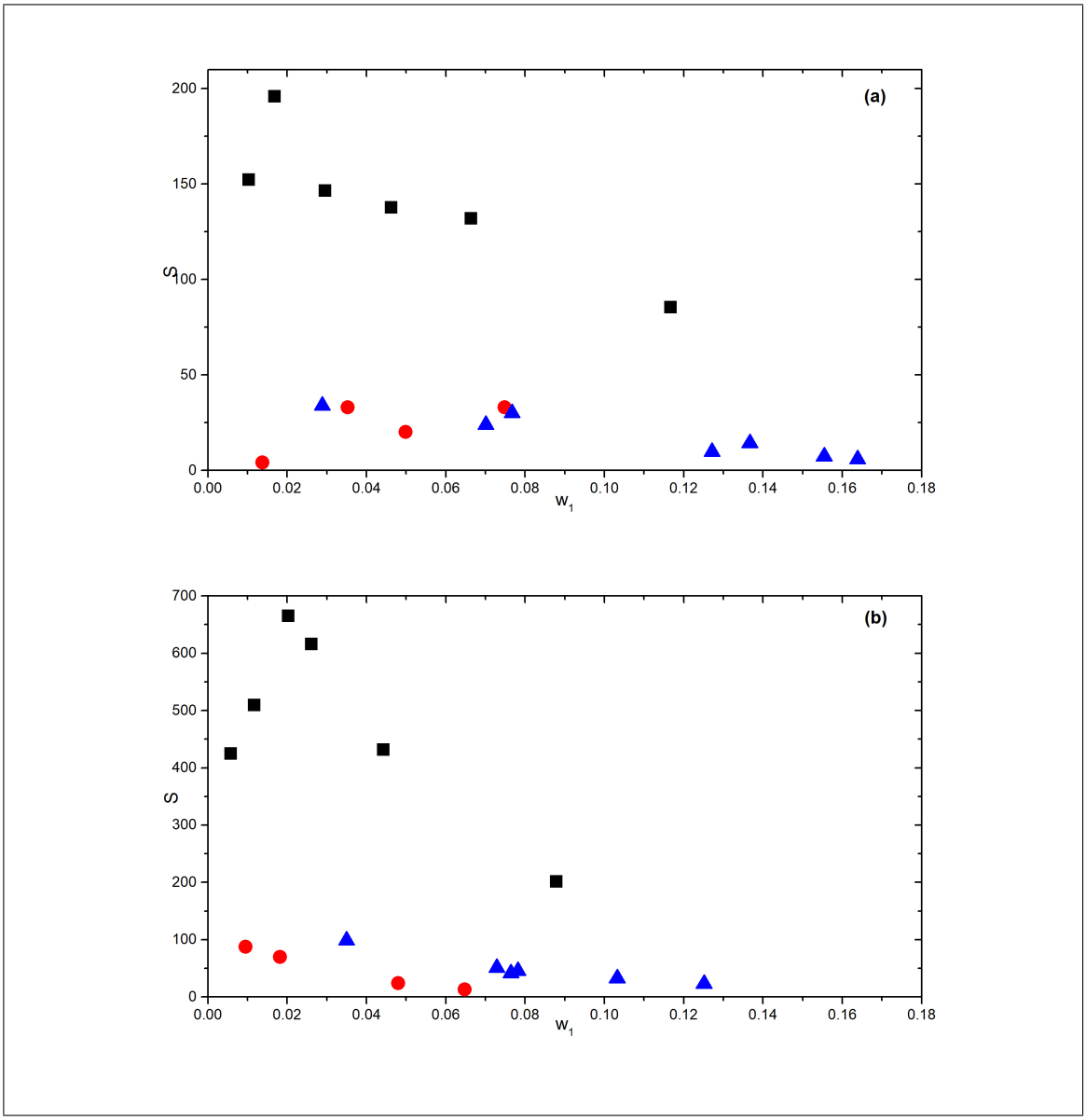

Figure 4.7. Selectivity of guaiacol in dodecane **(a)** and selectivity guaiacol in hexadecane **(b)**. Methanol (■), acetone (●), ethanol (▲)

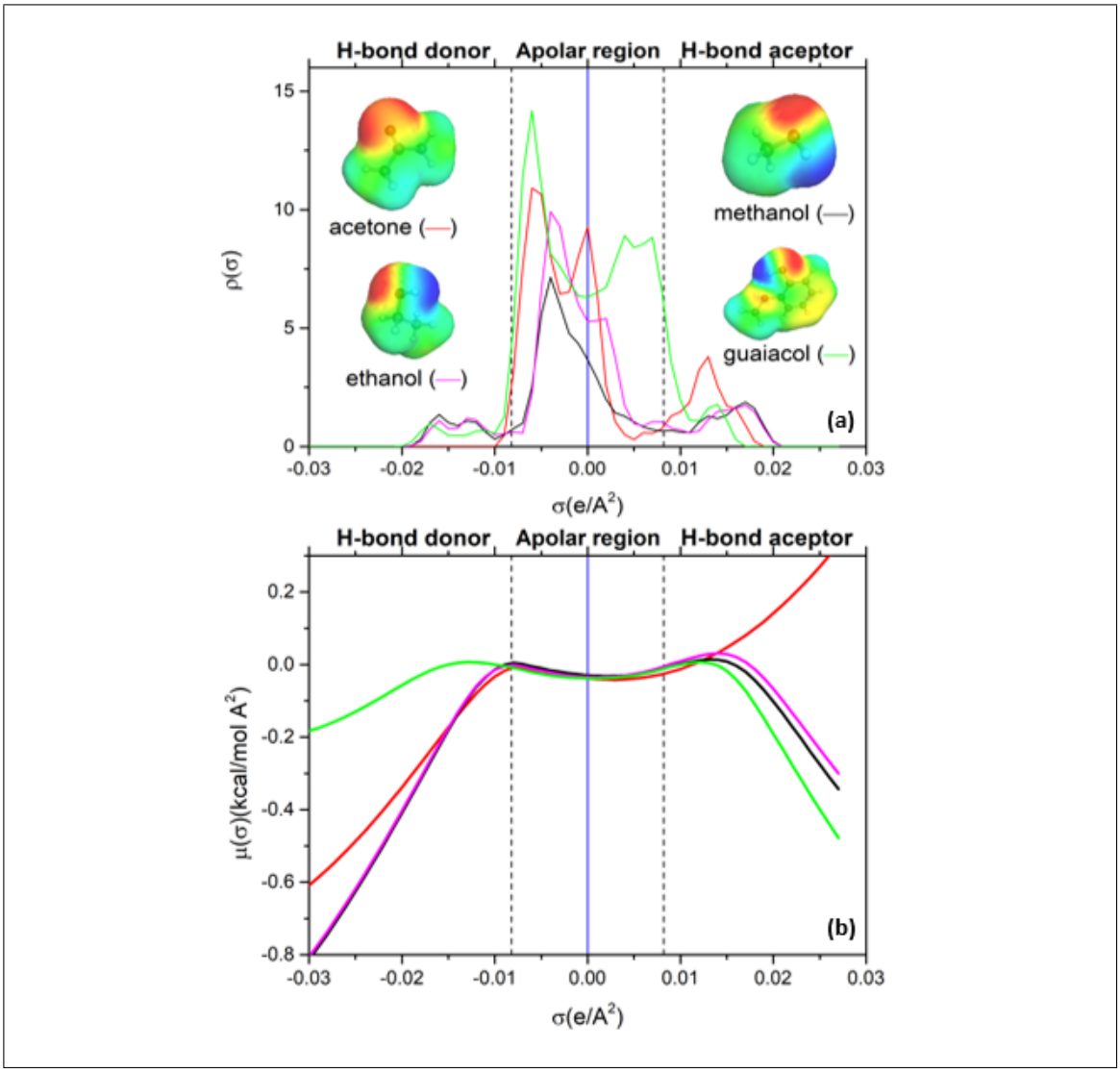

Figure 4.8. Sigma profile **(a)** and sigma potential **(b)**. Guaiacol (–), methanol (–), ethanol (–) and acetone (–).

5. CONCLUSIONS AND PERSPECTIVES

Excess volume, mixing density and viscosity for the systems guaiacol + methanol, guaiacol + ethanol and guaiacol + acetone were measured at five temperatures (298.15 to 333.15 K). The data related to guaiacol + methanol, guaiacol + ethanol and guaiacol + acetone are completely new. The data related to dodecane and hexadecane increase the available literatura knowledge of this systems, there are only a few data in the literature. In all cases, was able to show the behavior and was able to fit with a thermodynamic model. Binary liquid-liquid equilibrium data of guaiacol + dodecane, guaiacol + hexadecane, dodecane + methanol and hexadecane + methanol were also measured. In this case, the equilibrium behavior was measured at temperatures between 293.15 K and 328.15 K for the case of the dodecane equilibrium and between 293.15 K and 338.15 K for the mixture with hexadecane and 293.15 K and 333.15 K for the others, this measurements increase the available literature knowledge of this system. The experimental procedure that was applied for the binary systems allows the measurement of both the composition of the two liquid phases in equilibrium and the relative amounts of the two phases. In case of the ternary equilibrium, methanol is the best option to separated guaiacol from the phenolic phase.

It is expected that this work will serve as a basis for future research and applications that will increase the use of renewable energy. In addition, this research provides useful information to continue making ternary liquid-liquid equilibria and the separation simulations. It is important to understand the thermodynamic mixes behavior, so this work is expected to increase the scientific knowledge of the community.

REFERENCES

Amore, S., Horbach, J., & Egry, I. (2011). Is there a relation between excess volume and miscibility in binary liquid mixtures. *The Journal of chemical physics*, *134*(4).

Blanco, E., Sepulveda, C., Cruces, K., García-Fierro, J., Ghampson, I., & Escalona, N. (2019). Conversion of guaiacol over metal carbides supported on activated carbon catalysts. *Catalysis Today*.

Casás, L. M., Touriño, A., Orge, B., Marino, G., Iglesias, M., & Tojo, J. (2002). Thermophysical properties of acetone or methanol+ n-alkane (c9 to c12) mixtures. *Journal of Chemical & Engineering Data*, *47*(4), 887–893.

Demirbas, A. (2009). Biorefineries: current activities and future developments. *Energy Conversion and Management*, *50*(11), 2782–2801.

Eckert, F., & Klamt, A. C. (2010). Version c2. 1, release 01.11; cosmologic gmbh & co. *KG: Leverkusen, Germany*.

Elliott, D. C., Biller, P., Ross, A. B., Schmidt, A. J., & Jones, S. B. (2015). Hydrothermal liquefaction of biomass: developments from batch to continuous process. *Bioresource technology*, *178*, 147–156.

Gross, J., & Sadowski, G. (2001). Perturbed-chain saft: An equation of state based on a perturbation theory for chain molecules. *Industrial & engineering chemistry research*, *40*(4), 1244–1260.

Kang, S., Li, X., Fan, J., & Chang, J. (2013). Hydrothermal conversion of lignin: a review. *Renewable and Sustainable Energy Reviews*, *27*, 546–558.

Kislik, V. (2012). *Advances in development of solvents for liquid- liquid extraction.*

Elsevier: Amsterdam.

Ksiaczak, A., & Kosiński, J. J. (1990). Liquid-liquid equilibrium in binary polar aromatic+ hydrocarbon systems. *Fluid Phase Equilibria*, *59*(3), 291–308.

Lamsal, B. P., & Tyagi, R. (2010). Bioenergy and biofuel from biowastes and biomass..

Letcher, T. (1975). The excess volumes of some mixtures of saturated and unsaturated c6 hydrocarbons. *The Journal of Chemical Thermodynamics*, *7*(3), 205–209.

Müller, E., Berger, R., Blass, E., Sluyts, D., & Pfennig, A. (2000). Liquid–liquid extraction. *Ullmann's Encyclopedia of Industrial Chemistry*.

Palomar, J., Gonzalez-Miquel, M., Bedia, J., Rodriguez, F., & Rodriguez, J. J. (2011). Task-specific ionic liquids for efficient ammonia absorption. *Separation and purification technology*, *82*, 43–52.

Peterson, A. A., Vogel, F., Lachance, R. P., Fröling, M., Antal Jr, M. J., & Tester, J. W. (2008). Thermochemical biofuel production in hydrothermal media: a review of sub-and supercritical water technologies. *Energy & Environmental Science*, *1*(1), 32–65.

Prausnitz, J. M., Lichtenthaler, R. N., & de Azevedo, E. G. (1998). *Molecular thermodynamics of fluid-phase equilibria*. Pearson Education.

Renon, H., & Prausnitz, J. M. (1968). Local compositions in thermodynamic excess functions for liquid mixtures. *AIChE journal*, *14*(1), 135–144.

Sandler, S. I. (2017). *Chemical, biochemical, and engineering thermodynamics*. John Wiley & Sons.

Silva, N. K. G., Ribas, R. M., Monteiro, R. S., de Souza Barrozo, M. A., & Soares, R. R. (2020). Thermodynamic equilibrium analysis of the vapor phase hydrodeoxygenation of guaiacol. *Renewable Energy*, *147*, 947–956.

Sulman, A., Mäki-Arvela, P., Bomont, L., Alda-Onggar, M., Fedorov, V., Russo, V., ... others (2019). Kinetic and thermodynamic analysis of guaiacol hydrodeoxygenation. *Catalysis Letters*, *149*(9), 2453–2467.

Upton, B. M., & Kasko, A. M. (2015). Strategies for the conversion of lignin to high-value polymeric materials: review and perspective. *Chemical reviews*, *116*(4), 2275–2306.

Verma, M., Godbout, S., Brar, S., Solomatnikova, O., Lemay, S., & Larouche, J. (2012). Biofuels production from biomass by thermochemical conversion technologies. *International Journal of Chemical Engineering*, *2012*.

Walas, S. (2013). *Phase equilibria in chemical engineering*. Butterworth-Heinemann.

APPENDIX

Extraction of guaiacol from hydrocarbons as an alternative for the upgraded bio-oil purification: Experimental and computational thermodynamic study

Matías I. Campos-Franzani[a,b], Nicolás F. Gajardo-Parra[a], César Pazo-Carballo[c], Paulo Aravena[a], Rubén Santiago[d], José Palomar[d], Néstor Escalona[a,b,c,e], Roberto I. Canales[a,b,*]

[a] *Departamento de Ingeniería Química y Bioprocesos, Escuela de Ingeniería, Pontificia Universidad Católica de Chile, Avenida Vicuña Mackenna 4860, Macul, Santiago, Chile*
[b] *Millenium Nuclei on Catalytic Processes towards Sustainable Chemistry (CSC)*
[c] *Departamento de Química Física, Facultad de Química y de Farmacia, Pontificia Universidad Católica de Chile, Avenida Vicuña Mackenna 4860, Macul, Santiago, Chile*
[d] *Chemical Engineering Department, Universidad Autónoma de Madrid, 28049 Madrid, Spain*
[e] *Unidad de Desarrollo Tecnológico, Universidad de Concepción, Coronel, Chile*

Abstract

Guaiacol is an important lignin derivative used as an intermediate for obtaining high value-added molecules through heterogeneous catalysis. Typical solvents used in the catalytic conversion of guaiacol are dodecane and hexadecane. In order to understand the potential separation of guaiacol from the conversion mixture, three compounds were selected as potential extracting solvents: methanol, ethanol, and acetone. Thus, this study is divided in three parts. First, the measurement of the properties of the pure components involved in this work as density and viscosity. Second, the measurement of the density, viscosity, and liquid-liquid equilibrium of the binary systems, and third, the measurement of the liquid-liquid equilibrium of the ternary systems composed by guaiacol + (methanol, ethanol or acetone) + (dodecane or hexane). Pure component and binary mixtures properties were obtained at temperatures between 293.15 K and 333.15 K and the ternary systems at 313.15 K, all of them at 101.13 kPa. Phase equilibrium was modeled with NRTL, COSMO-RS, and COSMO-SAC. The results obtained suggest that methanol is the best extracting solvent of guaiacol due to its high selectivity, high affinity with the solute, and a wide liquid-liquid immiscibility with dodecane. Models selected in this work represent accurately the ternary system composed by guaiacol + methanol + (dodecane or hexadecane), so they can be chosen as potential tools for further process simulation of extraction and recovery of guaiacol.

Keywords: Guaiacol, Extraction, Bio-oil, Liquid-liquid equilibrium

*Corresponding author
Email address: rocanalesm@ing.puc.cl (Roberto I. Canales)

1. Introduction

The conversion of lignocellulosic biomass into biofuels, or other high-value chemicals, is a broadly studied process that reduces the greenhouse gas emissions and decreases the dependency on the oil industry[1]. Lignin is one of the main constituents of the lignocellulosic biomass and the source of several oxygenated hydrocarbons and aromatic condensates obtained through the transformation of biomass[2]. These lignin-derivative molecules are economically attractive as platform chemicals for producing fuels or other compounds of high added-value[3].

An efficient process for converting lignocellulosic biomass into bio-oil is the fast pyrolysis. This process generates a complex liquid mixture composed of a water-soluble fraction and a heavy water-insoluble fraction containing a vast number of molecules and chemical families; this mixture is the bio-oil. The heavy fraction includes the most varied and interesting compounds, for instance, phenols, aromatic hydrocarbons, ketones, etc., but its complexity requires the fractionation of those groups for further processing or purification[4]. Then, the step that should follow after the pyrolysis and the fractionation of the bio-oil is the catalytic upgrade. One of the ideas of the catalytic conversion of the bio-oil is to decrease the amount of oxygen in the mixture by transforming it in water, but keeping the carbon content in the upgraded bio-oil phase[5]. The direct catalytic conversion of bio-oil is still a very challenging process due to the rapid deactivation of the catalyst and the different reactivities shown by the molecules present in the multicomponent mixture. Thus, upgrading fractions of bio-oil or using model molecules is preferred for understanding the behavior of specific families of compounds [6].

There are reports of different reactions for upgrading the bio-oil like decarbonylation, decarboxylation, hydrocracking, etc., but hydrodeoxygenation (HDO) is one the most studied

techniques because it yields to liquid fuels, aromatic compounds or cycloalkanes [7]. Among the model bio-oil molecules typically used for studying HDO are phenols or methoxy substituted aromatics. Guaiacol and guaiacol-like compounds are some of the representative compounds of both families due to their relatively high concentration in the bio-oil [7]. Also, guaiacol shows a high conversion and selectivity into phenolic or aromatic compounds, such as phenol, cresol, benzene, toluene, etc., under certain conditions [8, 9]. Typical solvents used to carry out the HDO of guaiacol are long-chain hydrocarbons like dodecane or hexadecane [8, 10, 11, 12, 13]. However, some of the challenges after performing the HDO is the separation of high-value compounds formed in the multicomponent liquid phase, the removal of potential contaminants of the bio-fuel, and the recovery of the unreacted starting molecules.

Thermodynamic and physical data of bio-oil model molecules and their mixture with other solvents or components is essential for assessing their behavior in the reaction mixture and for studying their separation and purification. This information is relevant for validating models that are useful for effective process design and scale-up. There are several works reporting the fractionation of bio-oil into different group of compounds obtaining diverse guaiacol-type molecules among their fractions [14, 4]. However, there is not much information about the liquid-liquid extraction of guaiacol from a representative solvent using a selected extractant. For instance, Li et al. [15] report the extraction of guaiacol from a pyrolytic sugar, where guaiacol is a model contaminant of that mixture. Then, several ionic liquids are screened for the liquid-liquid separation of guiacol from a water phase. Also, Cesari et al. [16] and Stepan et al. [17] study the extraction of guaiacol from water using different solvents like choline bis(trufluoromethylsulfonyl imide), isopropyl acetate, and toluene, where the water + guaiacol mixture represents a model pyrolytic oil.

The objective of this work is to study the liquid-liquid extraction of guaiacol from do-

decane or hexadecane. Guaiacol represents the unreacted biomass model molecule after the catalytic HDO, and dodecane or hexadecane are the model reaction medium. Solvents selected for the guaiacol extraction were methanol, ethanol and acetone, since those are readily available, low viscosity and cheap solvents. Then, relevant physical and transport properties of the solute-solvent were first analyzed. Thus, density and dynamic viscosity measurements were performed for the binary mixtures composed by guaiacol + (methanol, ethanol, or acetone) between 293.15 K and 333.15 K at 101.3 KPa. Density values were used for calculating the excess molar volumes (V^E) of the previous mixtures to assess their configurational arrangement in the liquid phase. Then, liquid-liquid equilibrium (LLE) measurements of the binary mixtures composed of guaiacol + (dodecane or hexadecane) were performed between 293.15 K to 338.15 K at 101.3 kPa. Finally, the LLE measurements for the ternary systems composed by guaiacol + (methanol, ethanol or acetone) + (dodecane or hexadecane) were performed at 313.15 K and 101.13 kPa, as key thermodynamic information for extraction operation design. The excess volumes were correlated with Redlich and Kister. LLE results were modeled with NRTL, COSMO-RS, and COSMO-SAC, opening the opportunity for future conceptual separation design by process simulation.

2. Materials and methods

2.1. Materials

The compounds used in this work were guaiacol(1), dodecane(2), hexadecane(3), methanol(4), ethanol(5) and acetone(6). The details about these components are shown in Table 1 with their respective molar mass, CAS number, supplier, type and purities. All of them were used from the same batch as received without any futher purification.

Table 1: Specifications of chemicals used in this work as molar mass (M), CAS number, supplier, type, and purity

Fluid	M (g·mol^{-1})	CAS number	Supplier	Type	Purity (wt%)
guaiacol	124.14	90-05-1	Sigma-Aldrich	For Synthesis	≥99.0
dodecane	170.34	112-40-3	Merck	For Synthesis	≥99.0
hexadecane	226.45	544-76-3	Merck	For Synthesis	≥99.0
methanol	32.04	67-56-1	Acros Organics	AcroSeal Extra dry	≥99.9
ethanol	46.07	64-17-5	Acros Organics	AcroSeal Extra dry	≥99.5
acetone	58.08	67-64-1	Merck	SupraSolv	≥99.0

2.2. Density (ρ) and viscosity (η) measurements

Density and dynamic viscosity of pure compounds and mixtures were measured in an Anton Paar DMA4500M Densitometer (Graz, Austria) connected to an Anton Paar Lovis 200ME microviscometer (Graz, Austria). The densitometer consists of a vibrating U-tube to measure the density with a reported accuracy of 0.00005 g·cm^{-3}. The temperature inside the tube is measured with a Pt-100 thermometer with an accuracy of 0.01 K. The densitometer was calibrated with double distilled deionized and degassed water, and dry air at a pressure of 101.3 kPa. The dynamic viscosity measurements were performed in a microviscomenter that holds a temperature controlled capillary of 1.59 mm of inside diameter. The technique for measuring the viscosity is the falling ball principle. The ball falling inside the capillary, which at the same time contains the liquid sample in its interior, has a known density. The equipment automatically measures the time that the falling ball takes to pass between two points of the capillary at a certain angle for at least ten times. The viscosity is calibrated with the standards provided by the manufacturer. Viscosity measurements have a reported accuracy of 0.17%.

2.3. Liquid-liquid measurements

LLE measurements were performed for binary and ternary systems of known feed compositions. All the mixtures were added gravimetrically to a jacketed glass cell using an

analytical balance (Sartorius Practum 224-1s, Germany) with a repeatability of 0.1 mg. The equilibrium cell, that also contained a magnetic stir bar inside, was placed over a stir plate and connected to a thermoregulated water circulator for keeping the temperature of the mixture constant during the experiment. A RTD platinum thermometer (VWR® Traceable®, ± 0.1 K) was placed in the top of the cell until the thermocouple touched the liquid mixture for controlling the temperature during the mixing and settling process. The mixture was stirred for 4 hours and then it was left to stand for at least 12 hours or until observing two clear liquid phases before sampling. Aproximately 0.5 mL samples of the upper and lower phases were taken with a syringe, weighed and dissolved with a known mass of chloroform before their analysis. The samples were analyzed with a gas chromatograph (Shimadzu Nexis GC-2030) equipped with a flame ionization detector, split-splitless injector and a Elite 1 capillary column 100% dimethyl polysiloxane (30 m × 0.53 mm × 3.0 μm) with a flow rate of 15 $cm^3 \cdot min^{-1}$ of nitrogen used as the carrier gas. The temperature program include an isothermal analysis at 310 K, which lasted 3 min. Then a ramp of 10 K$\cdot$ min^{-1} was used to increase temperature to 523 K. The external standard method was used to quantify the amount of each compound in the mixture. The analysis was performed at least three times for each of the three samples taken from both phases. A series of LLE data was obtained by changing the temperature in the case of the binary systems and the feed composition at constant temperature in the case of ternary systems.

3. Thermodynamic modeling

All the liquid-liquid experimental results reported in this work were calculated using three thermodynamic models implemented in Aspen Plus© V10, i.e. NRTL[18], COSMO-RS [19] and COSMO-SAC [20]. To evaluate the accuracy of the thermodynamic models compared with the results presented in this work, the root-mean-square deviation (RMSD)

was calculated according to Equation 1, given by

$$\mathrm{RMSD} = \sqrt{\frac{\sum_{n=1}^{N} \left(\hat{y}_n - y_n\right)^2}{N}} \tag{1}$$

where N represents the total number of experimental points modeled, $\hat{y}_n$ is the calculated value and y_n is the experimental value.

Liquid-liquid calculations for the binary and ternary systems using NRTL and the COSMO-based models implemented in Aspen Plus© were obtained from the γ-γ isofugacity scheme as shown in Equation 2:

$$x_i^{\mathrm{I}} \gamma_i^{\mathrm{I}} = x_i^{\mathrm{II}} \gamma_i^{\mathrm{II}} \tag{2}$$

where indices I and II denote the two liquid phases, x_i are the mole fractions of component i in each liquid phase, and γ_i are the activity coefficients computed by NRTL, COSMO-RS or COSMO-SAC.

3.1. NRTL

Binary and ternary LLE mixtures were correlated using the non-random two liquid model (NRTL). Activity coefficients are calculated with NRTL according to Equation 3:

$$\ln \gamma_i = \frac{\sum_j x_j \tau_{ji} G_{ji}}{\sum_k x_k G_{ki}} + \sum_j \frac{x_j G_{ij}}{\sum_k x_k G_{kj}} \left(\tau_{ij} - \frac{\sum_m x_m \tau_{mj} G_{mj}}{\sum_k x_k G_{kj}} \right) \tag{3}$$

where τ_{ij} and τ_{ji} are the adjustable parameters. They can be set as temperature dependent or independent by adjusting a_{ij}, b_{ij}, e_{ij} and f_{ij} parameters of Equation 4. The non-randomness parameter (α_{ij}) is kept constant for all the binary pairs in 0.2, with the exception of the dodecane + ethanol mixture where α_{ij} was fixed in 0.3. G_{ij} values calculated according to Equation 5.

Table 2: Constants for calculating binary NRTL parameters with Equation 4

Component	NRTL parameters						
	a_{ij}	a_{ji}	b_{ij}	b_{ji}	α_{ij}	e_{ij}	e_{ji}
guaiacol/dodecane	4.679	-8.740	-553.09	2818.99	0.2		
guaiacol/hexadecane	2.999	-7.296	129.14	2373.76	0.2		
guaiacol/methanol	-2.163	2.372	0	0	0.2		
guaiacol/ethanol	0.028	0.163	0	0	0.2		
guaiacol/acetone	1.036	-1.865	0	0	0.2		
dodecane/methanol	-2.939	0.194	1276.33	966.66	0.2		
dodecane/ethanol	0.066	2.678	0	0	0.3		
dodecane/acetone	0.025	1.388	0	0	0.2		
hexadecane/methanol	-48.089	118.308	2407.19	-3165.90	0.2	7.8697	-18.6726
hexadecane/ethanol	-8.162	2.689	2646.73	91.6329	0.3		
hexadecane/acetone	0.028	1.897	0	0	0.2		

$$\tau_{ij} = a_{ij} + b_{ij}/T + e_{ij} \ln T \tag{4}$$

$$G_{ij} = \exp\left(-\alpha_{ij}\tau_{ij}\right) \tag{5}$$

Parameters τ_{ij} and τ_{ji} are fit to experimental binary or ternary LLE data obtained in this work or from literature in specific cases. All the parameters for Equation 4 are shown in Table 2. Parameters for the systems that form liquid-liquid immiscibility, i.e., guaiacol + dodecane, guaiacol + hexadecane, and dodecane + methanol were fit to data from this work at different temperatures. Parameters for the system hexadecane + ethanol were fit from Hwang et al.[21], and for hexadecane + methanol retrieved from Aspen Plus© V10 database. Parameters for all the other binary pairs were fit to ternary liquid-liquid equilibrium data from this work, since they are completely miscible.

3.2. COSMO based models

COSMO-RS is a predictive activity coefficient model developed by Klamt and coworkers [22] that uses quantum chemical calculations for obtaining a σ-profile as an input for calculating different thermodynamic properties. COSMO-SAC is a reimplementation of COSMO-RS proposed by Sandler and coworkers [20, 23], but the same σ-profiles can be used for the thermodynamic calculations.

In this work, σ-profiles for dodecane, hexadecane, methanol, ethanol, and acetone were obtained from the COSMOthermX (version C3.0 Release 18.0)[24] software database. The σ-profile for guaiacol, methanol, ethanol, and acetone were optimized using the quantum chemical software Turbomole[25] for obtaining a stable molecular geometry and for generating its corresponding *.cosmo file at BP86/TZVP computational level. Then, all the σ-profiles were used in Aspen Plus© V10 for calculating the LLE of the binary and ternary systems reported in this work using COSMO-RS and COSMO-SAC. For compounds with more than one conformation available, all of them were considered for the calculations, selecting those that gave the better results compared with experimental data.

4. Results

4.1. Density and dinamic viscosity of pure compounds

Density ($g \cdot cm^{-3}$) and dynamic viscosity (mPa·s) measurements of pure compounds used in this work are reported in Table A.1 at temperatures between 293.15 K and 333.15 K and a pressure of 101.3 kPa. The results are in agreement with literature data for density of guaiacol [26, 27, 28], dodecane [29, 30, 31, 32, 33], hexadecane [34, 35, 36, 37, 38], methanol [39, 40, 41], ethanol [42, 43, 44] and acetone [45, 46, 47]. Density data for the pure components were fit to Equation 6. Densities calculated with Equation 6 have RMSDs below $2.3 \cdot 10^{-3}$ $g \cdot cm^{-3}$. The experimental data from this work, from literature, and

fitting results are presented in Figure 1(a). The density decreases linearly by increasing the temperature for all the pure components reported in this work. This is the expected behavior because at higher temperatures there is a higher free volume and distance between molecules. The oxygenated compounds have the higher density because their stronger intermolecular interactions produce a lower free volume compared with the alkanes. Density follows the next tendency: guaiacol > methanol > acetone > ethanol > hexadecane > dodecane. All of the guaiacol extracting solvents, i.e. methanol, ethanol and acetone, have a higher density than either dodecane or hexadecane. This is a good feature for the selective extraction of guaiacol, since this compound is also more dense than the alkanes. If the solvent have a good selectivity for guaiacol, the extracting solvent-rich phase will go to the lower phase and the exhausted alkane will stay in the upper phase.

$$\rho(T) = a + bT \tag{6}$$

Viscosities measured in this work are compared to the literature data available for guaiacol [28], dodecane[29, 30, 31, 32, 33], hexadecane [34, 35, 36, 37, 38], methanol [48, 49, 50], ethanol [51, 52, 53] and acetone [54, 55]. The experimental measurements and comparison with literature are shown in Figure 1(b). Viscosity data was fitted to the Vogel-Fulcher-Tamman (VFT) shown in Equation 7, where A, B and T_0 are the VFT fitting parameters with values reported in Table A.3. RMSD for pure viscosity calculations are between $1{\cdot}10^{-4}$ mPa·s to $3.1{\cdot}10^{-3}$ mPa·s. VFT fitting line is also shown in Figure 1(b).

$$\eta_{VFT}(T) = A \exp\left(\frac{B}{T - T_0}\right) \tag{7}$$

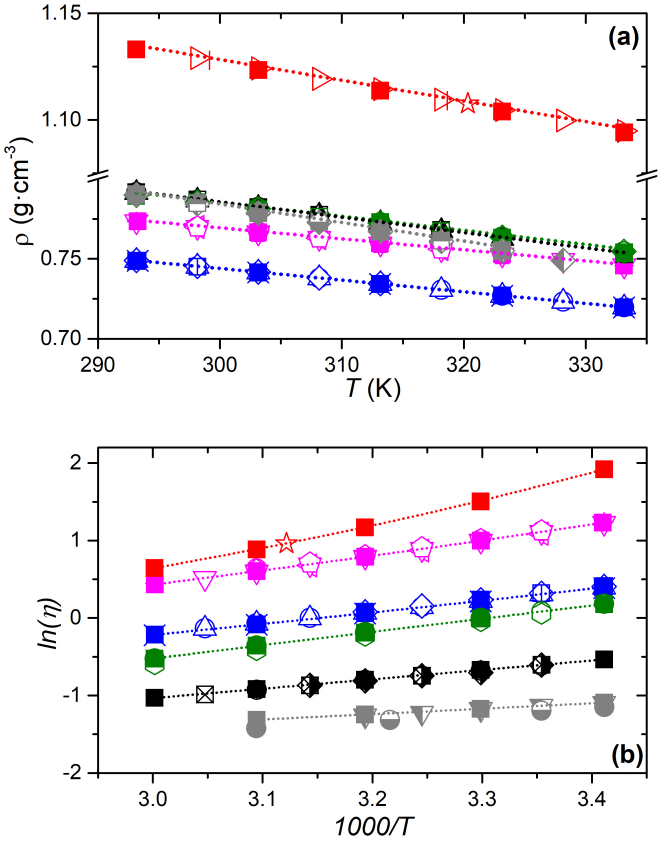

Figure 1: **(a)** Density (g·cm^{-3}) as a function of temperature and **(b)** logarithm of dynamic viscosity as a function of 1000 times the inverse temperature of guaiacol (■), dodecane (■), hexadecane (■), methanol, (■) ethanol (■), and acetone (■) at a pressure of 101.3 kPa. Comparison with data reported from Cunha et al.[26](▷), Newton et al.[28](☆),Jaeger et al.[27](|), Dai et al.[29](○), Zhao et al.[30](△), Zhang et al.[56](◫), Luninng Prak et al.[32](×), Liu and Zhu[33](◇), Sirbu et al.[34](◁), Luning Prak et al.[35](+), Aissa et al.[36](▽), Wang et al.[37](⬠), Esteban et al.[38](|), Smyth et al.[42](⊖), Khimenko et al.[43](⊞), Tashima et al.[44](⟠), Misra et al.[51](◑), Tommila et al.[52](⊙), Garcia et al.[53](⬠, Long et al.[39](◐), Gonfa et al.[40](◧), Varfolomev et al.[41](◭), Saha et al.[48](⬗), Rauf et al.[49](⊠), Mikhail et al.[50](⏀), Enders et al.[46](⬖), Estrada et al.[45](⬒), Krakowiak et al.[47](◒), Yang et al.[54](◸), Howard et al.[55](◓). Dotted line (···) represents the fitting with Equation 6 with parameters reported in Table A.2 and VFT model from Equation 7 with parameters reported in Table A.3 for viscosity.

In general, viscosity decreases exponentially by rising the temperature. Thus, viscosity correlations, as VFT, show that the logarithm of the viscosity is linear function of the inverse temperature[57]. A high viscosity is related with a stronger intermolecular friction

produced by intermolecular interactions and a low free volume [58]. The viscosity follows the next tendency: guaiacol > hexadecane > dodecane > ethanol > methanol > acetone. Thus, the extracting solvents, have a lower viscosity compared with the alkanes. Then, they serve for decreasing the viscosity of guaiacol when mixed with each one. However, all the viscosities are below 10 mPa·s. Thus, the ternary LLE is expected to be reached in a short time due to the low mass transfer restrictions.

4.2. Mixture densities and excess molar volume

Guaiacol was observed to be completely miscible with methanol, ethanol and acetone between 293.15 K and 333.15 K. Then, density measurements of mixtures composed by guaiacol + (methanol, ethanol, or acetone) were obtained between in the same range of temperatures (up to 323.15 K in the case of acetone) at 101.3 kPa in the full range of compositions. To assess the non-ideal behavior of the mixtures, V^E was calculated using Equation 8 as follows:

$$V^{\mathrm{E}} = \frac{x_1 M_1 + x_2 M_2}{\rho} - \left(\frac{x_1 M_1}{\rho_1}\right) - \left(\frac{x_2 M_2}{\rho_2}\right) \tag{8}$$

where x_i, ρ_i and M_i are the composition, density and molecular weight of the compound i, respectively and ρ is the density of the mixture. Density and V^E data for the three binary mixtures are shown in Table A.2 and Figures A.1 and 2, respectively. V^E were fitted with the Redlich-Kister (RK) correlation:

$$V^{\mathrm{E}}_{RK} = x_1 \cdot x_2 \cdot \sum_{i=0}^{k} C_i \cdot \left(x_1 - x_2\right)^i \tag{9}$$

where C_i are the parameters of the correlation and x_i are the molar fractions of the components. RK parameters are shown in Table A.5 along with their RMSD ranging from 0.005 and 0.035 $cm^3 \cdot mol^{-1}$. Figure 2(a) shows the V^E of the binary mixture of guaiacol +

metanol, Figure 2(b) guaiacol + ethanol and Figure 2(c) guaiacol + acetone, as a function of the mole fraction of guaiacol, and the RK calculated curves.

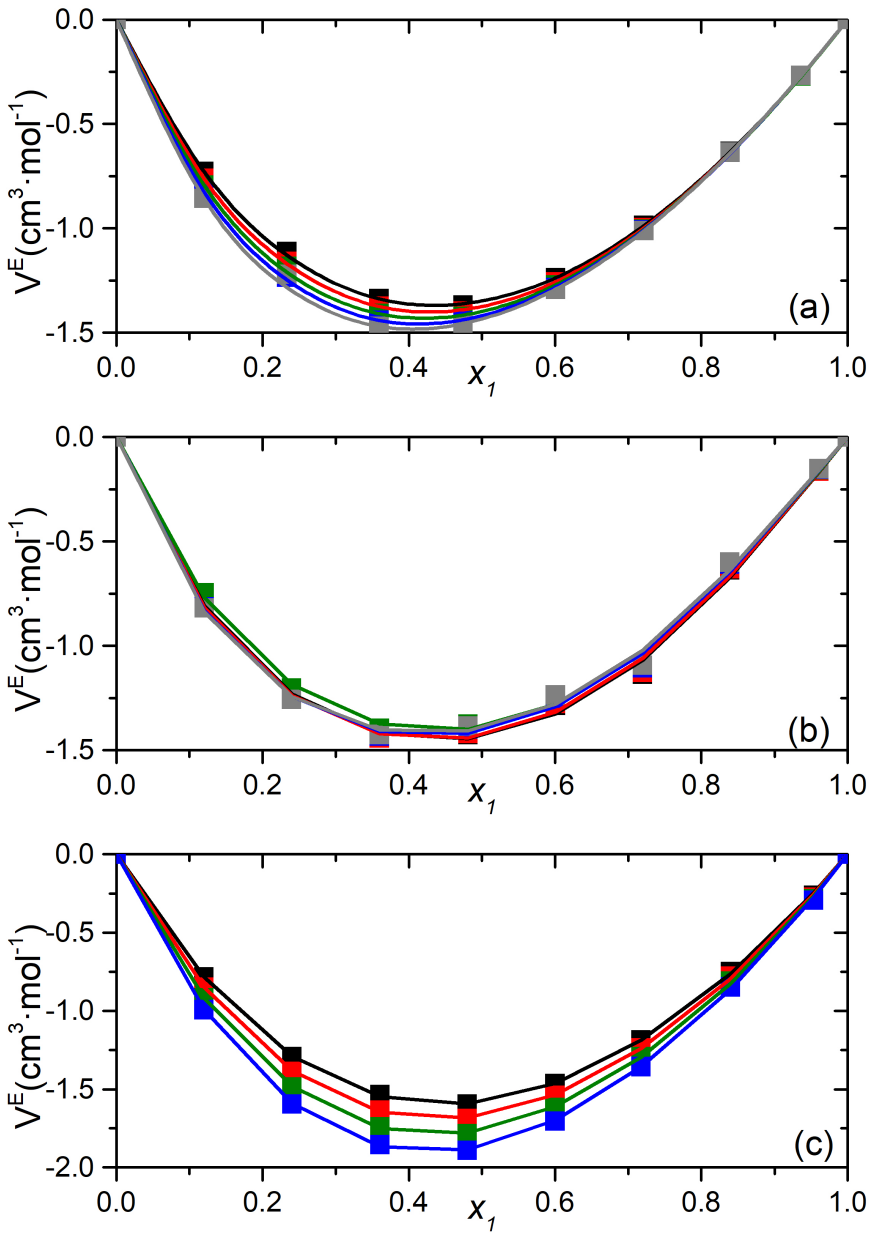

Figure 2: Excess molar volume ($cm^3 \cdot mol^{-1}$) in terms of the mole fraction of guaiacol for the binary mixtures composed of **(a)** guaiacol + methanol, **(b)** guaiacol + ethanol and **(c)** guaiacol + acetone at a pressure of 101.3 kPa and different temperatures: 293.15 K (■), 303.15 K (■), 313.15 K (■), 323.15 K (■), and 333.15 K (■). The continuous line represents the fitting with Redlich-Kister from Equation 9 using parameters reported in Table A.5

For three cases the mixture densities increase by adding guaiacol and by decreasing the temperature, as expected. All the V^E are negative, which can be explained because the intermolecular interactions between the small polar molecules with the guaiacol are stronger than the pure guaiacol-guaiacol interactions. Thus, unlike molecules can accomodate in the interstitial space between them, decreasing the total volume of the mixture as compared with the ideal volume. Also, a longer carbon chain in the alcohols produces a slightly more negative V^E. In the case of the acetone, it can be observed that the V^E is more negative compared with the alcohols because the interaction guaiacol-acetone is stronger. There is a very small temperature effect on the V^E for the systems with both alcohols but in acetone is observed that a more negative V^E is produced at higher temperatures.

The density of mixtures is an important property for determining the operation volume of the equipment where the liquid-liquid separation will occur or how the phase separation will be distributed.

4.3. Mixture viscosity

Figure 3 and Table A.3 show experimental data measured in this work of the viscosities of the miscible binary systems composed by guaiacol + (methanol, ethanol, or acetone). Measurements were performed as a function of the composition of guaiacol at temperatures between 293.15 K and 333.15 K and a pressure of 101.3 kPa. This data was correlated using Equation 10, given by:

$$\ln \eta_{mix} = x_i \ln \eta_i + x_j \ln \eta_j + 2k_{ij} x_i x_j \tag{10}$$

where η_{mix} is calculated viscosity of the mixture, η_i and η_j the viscosity of the pure components i and j at a fixed temperature, respectively. Also, x_i and x_j are the molar compositions of compounds i and j, respectively. Finally, parameter k_{ij} was adjusted to

experimental data with values of 2.33421 for guaiacol + methanol, 1.33704 for guaiacol + ethanol, and 2.28406 for guaiacol + acetone. Lines calculated with Equation 10 are shown in Figure 3 along with the experimental values.

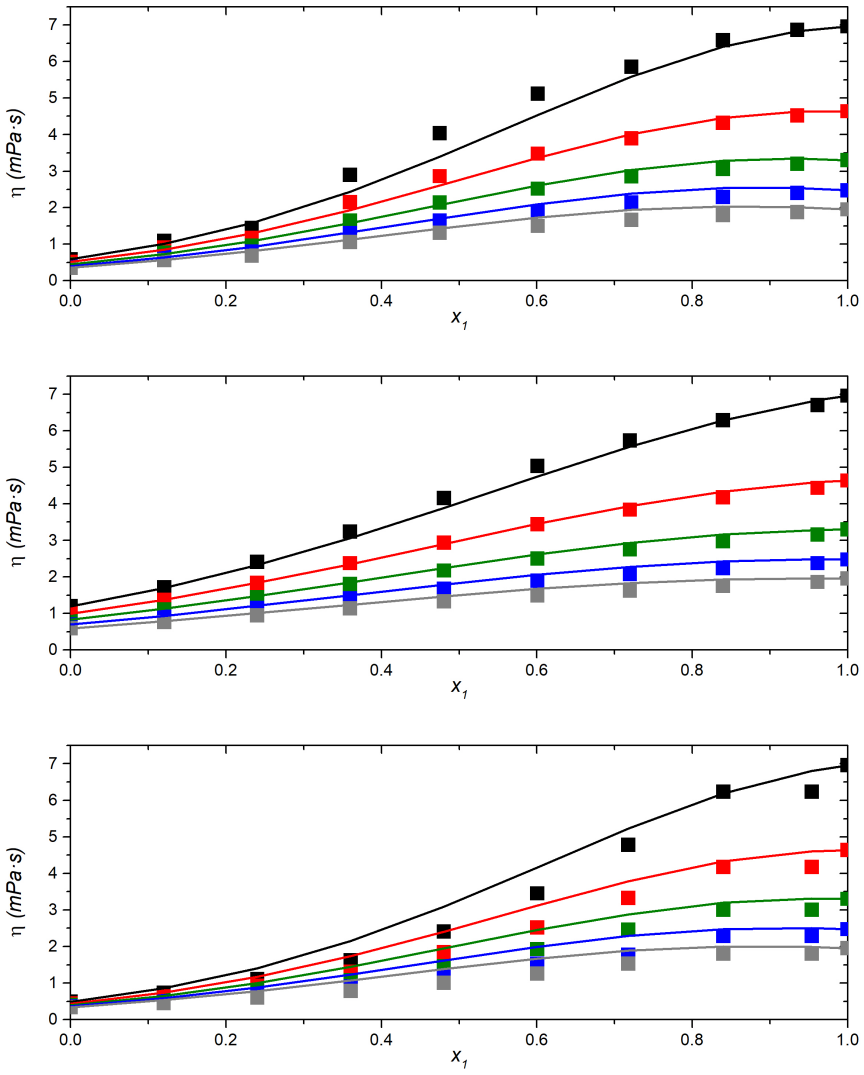

Figure 3: Dynamic viscosity (mPa·s) in terms of the mole fraction of guaiacol for the binary mixtures of **(a)** guaiacol + methanol, **(b)** guaiacol + ethanol and **(c)** guaiacol + acetone at a pressure of 101.3 kPa and different temperatures: 293.15 K (■), 303.15 K (■), 313.15 K (■), 323.15 K (■), and 333.15 K (■).The continuous line (-) represents the mixture viscosity calculation with Equation 10.

231 The viscosity decreases by increasing the temperature and increases by adding guaiacol,

as expected, since pure guaiacol has a higher viscosity compared with all the extracting solvents. This data is useful for estimating the viscosity of the liquid-liquid lower phase formed after the guaiacol extraction because this phase will be further processed for separating the solvent from guaiacol. However, as mentioned before, all the compounds considered in this work have a very low viscosity. Then, viscosity should not be an issue for the equilibrium rate of the LLE or for extracting the guaiacol + solvent phase for the next separation step.

4.4. Binary Liquid-Liquid equilibrium

Experimental binary LLE measurements were performed for those pairs of mixtures with scarce information in literature, for understanding the binary LLE behavior of the mixtures reported in the next section at 313.15 K, and for fitting binary interaction parameters for NRTL. LLE for the binary systems measured in this work are guaiacol + dodecane, guaiacol + hexadecane, dodecane + methanol, and hexadecane + methanol at temperatures ranging from 293.15 K to 338.15 K at 101.3 kPa. All the measurements are reported in Figure 4 in mass fraction along with their comparison with literature and NRTL, COSMO-RS and COSMO-SAC modeling. Also, our data is presented in Table A.4. The binary system composed by guaiacol + dodecane was not found in literature for comparison. Guaiacol + hexadecane LLE was compared with Ksiączak and Kosiński[59] observing a good agreement in the guaiacol-rich phase but with differences in the hexadecane-rich phase. This could be attributed to different errors associated with the experimental techniques, i.e. visual technique used by those authors versus sampling with GC used in this work, the purities of the solvents, etc. However, this binary mixture was prepared for this study at different guaiacol/hexadecane ratios and observed at 343 K (above the upper critical solution temperature (UCST) reported by Ksiączak and Kosiński[59]) but always observing the formation of two phases. LLE measurements of dodecane + methanol and hexadecane + methanol are also compared with literature with those points that are in our temperature range showing a

good agreement within our experimental error [60, 61, 62]. The system formed by ethanol + dodecane shows partial miscibility but its UCST is about 287 K [63, 64]. Then, this system is completely miscible in our range of temperatures. The system composed by hexadecane + ethanol also shows LLE behavior with a USCT around 327 K. This mixture has several measurements in literature with a clear coexistence curve and partially covering our temperature range [65, 63]. Finally, the binary mixtures composed by dodecane + acetone are completely miscible [60, 66] over 288.15 K and hexadecane + acetone shows an UCST at about 300 K [66]. Mixtures between dodecane and hexadecane or any combination of methanol, ethanol, and acetone are not of the interest of this work since they are not put together in the ternary system shown in the next section.

NRTL shows the best representation of the LLE binary systems compared with COSMO-RS and COSMO-SAC, as observed in Table 3, because binary systems were correlated with NRTL, and results from COSMO-based models are completely predictive. The guaiacol-rich phase is well represented by the three models for the guaiacol + dodecane and guaiacol + hexadecane mixtures, as observed in Figures 4(a) and 4(b), respectively. However, COSMO-SAC has a small overestimation of the composition of guaiacol when temperature increases. In the alkane-rich phase, COSMO-RS and COSMO-SAC show a large underestimation of the guaiacol composition assuming an almost guaiacol-free alkane phase. Therefore, the low accuracy of the alkane-rich phase is the main influence on the high RMSD of the calculations performed by COSMO-RS and COSMO-SAC. In the methanol + dodecane and methanol + hexadecane binary LLE systems there is a good representation of the alkane-rich phase by the three models and there is a small underestimation of the composition of methanol in the methanol-rich phase by COSMO-RS and COSMO-SAC. However, RMSD values obtained with COSMO-based models are below 0.06, which is a very accurate predictive result.

A low miscibility of the extracting solvent with the solvent media containing the solute,

i.e., (methanol, ethanol, or acetone) + (dodecane or hexadecane), is desired for avoiding the use of large amounts of solvent for recovering a specific solute, in this case guaiacol, and the complications that can generate the recovery of the same solvent. Methanol appears as a good candidate under this perspective because its large immiscibility gap with dodecane and hexadecane. Ethanol also shows a partial miscibility with hexadecane, but a LLE is observed at lower temperatures when mixed with dodecane. Since acetone is completely miscible with dodecane and hexadecane at most of the temperatures above 293.15 K, it looks disadvantageous compared with methanol. However, the better extracting solvent is better understood when the ternary system is studied in terms of selectivity and distribution ratio.

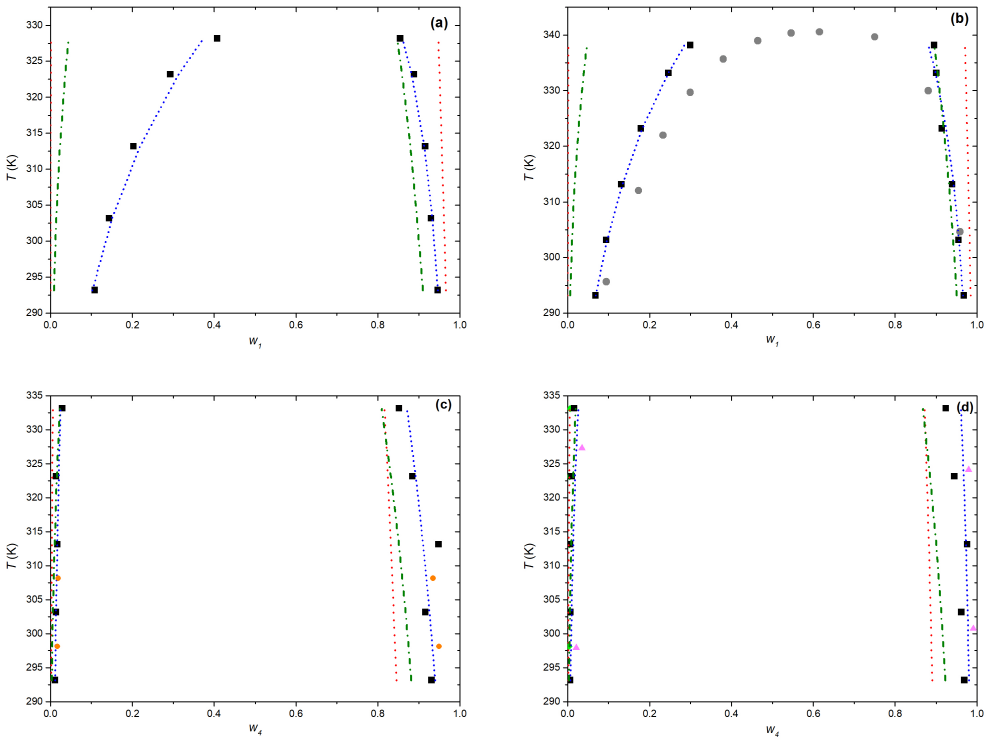

Figure 4: Experimental data (■) of liquid-liquid phase equilibria diagram of binary systems of **(a)** guaiacol + dodecane, **(b)** guaiacol + hexadecane, **(c)** methanol + dodecane and **(d)** methanol + hexadecane. Comparison with data reported by Kiza et al. [59](●), Casas et al. [60](●), Rogalski et al.(◆) and Stryjek et al.(▲) . The blue dotted line (···) represents represents the NRTL, red dash line (--) represent COSMO-SAC and green dash doted line (-·-) represent COSMO-RS model.

4.5. Ternary Liquid-Liquid equilibrium

Ternary LLE measurements were performed for the systems guaiacol + (methanol, ethanol, or acetone) + (dodecane or hexadecane) at 313.15 K and 101.3 kPa. Experimental results are shown in Table S5 and Figure 5 in mass fraction. No ternary data was found in literature for comparison purposes. The ternary systems of guaiacol + methanol + (dodecane or hexadecane) show a large immiscibility area forming one phase of almost pure alkane and the other mainly with the extracting solvent with guaiacol. This behavior is the

Table 3: Root mean square deviations (RMSD) of the model calculations of the binary liquid-liquid equilibrium systems measured in this work

Binary Systems			
	NRTL	COSMO-SAC	COSMO-RS
guaiacol/dodecane	0.0141	0.1842	0.1621
guaiacol/hexadecane	0.0070	0.1381	0.1136
dodecane/methanol	0.0144	0.0577	0.0440
hexadecane/methanol	0.0157	0.0532	0.0416
hexadecane/ethanol*	0.0105	0.1160	0.1050

* data from Hwang et al. [21]

expected since guaiacol can be extracted from the alkane at basically any compositions. A similar behavior but with a smaller immiscibility area is observed when guaiacol is extracted from hexadecane using ethanol. However, the hexadecane-rich phase contains up to about 17 wt% of ethanol when there is a low concentration of guaiacol. The systems containing ethanol + dodecane or acetone + (dodecane or hexadecane) show that are less convenient for guaiacol because the small LLE area and the solute cannot be extracted when present in low concentrations.

Ternary LLE results were also modeled with NRTL, COSMO-RS and COSMO-SAC as shown in Figure 5 with RMSDs reported in Table 4. Again, the correlative NRTL shows the best modeling results with the highest RMSD in 0.0332. COSMO-RS and COSMO-SAC show the best predictive results for the ternary mixture of guaiacol + methanol + (dodecane + hexadecane) with RMSDs between 0.0367 and 0.0624. These results are good if COSMO-RS and COSMO-SAC are intended for representing these mixtures in a further process simulation of the extraction and recovery of guaiacol.

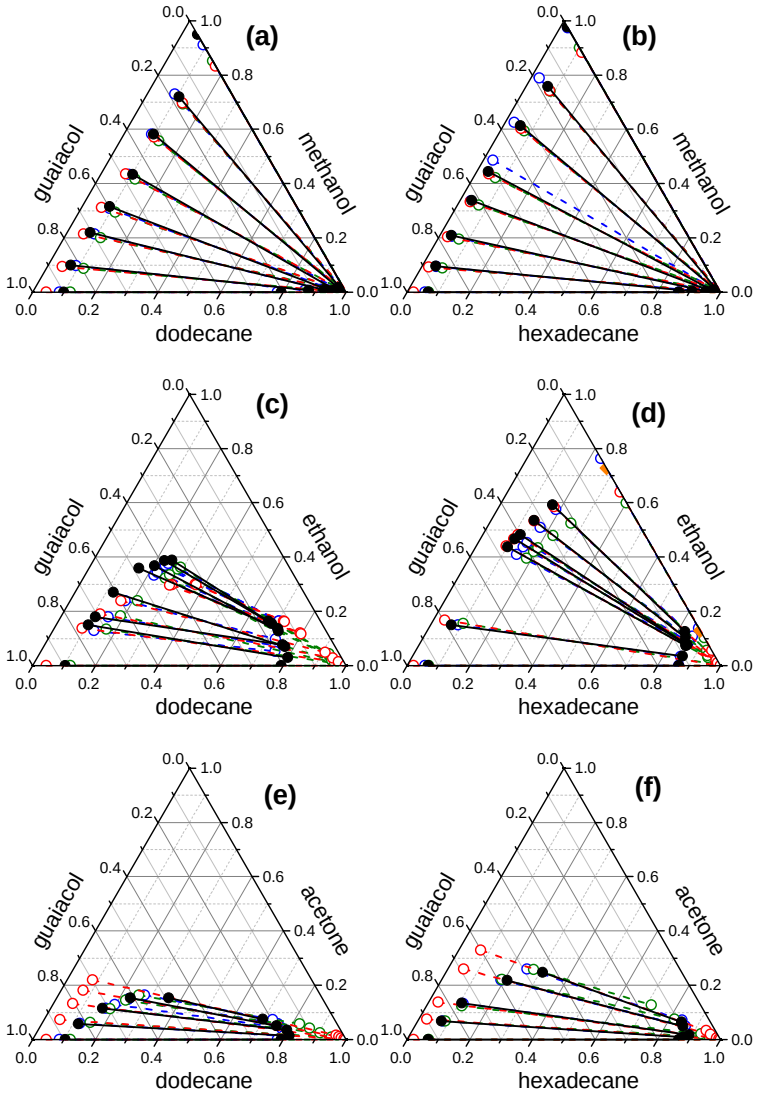

Figure 5: Liquid - liquid equilibrium of the ternary mixture of **(a)** guaiacol + dodecane + methanol, **(b)** guaiacol + hexadecane + methanol, **(c)** guaiacol + dodecane + ethanol, **(d)** guaiacol + hexadecane + ethanol, **(e)** guaiacol + dodecane + acetone, **(f)** guaiacol + hexadecane + acetone at 313.15 K in mass fraction. Experimental data (●), NRTL (○), COSMO-RS (○), COSMO-SAC(○) and Matsuda et al.[67](◆)

313 Another way to analyze the ternary systems and the best candidates for extracting

Table 4: LLE root mean square deviations (RMSD) for the models used in this work

Ternary Systems			
	NRTL	COSMO-SAC	COSMO-RS
guaiacol/dodecane/methanol	0.0332	0.0624	0.0540
guaiacol/hexadecane/methanol	0.0132	0.0431	0.0367
guaiacol/dodecane/ethanol	0.0278	0.0884	0.1144
guaiacol/hexadecane/ethanol	0.0202	0.0739	0.0656
guaiacol/dodecane/acetone	0.0223	0.1613	0.2164
guaiacol/hexadecane/acetone	0.0316	0.0995	0.1794

guaiacol from dodecane or hexadecane is the calculation of the distribution factor ($D_{i,w}$) shown in Equation 11, which is the mass fraction of compound i in the guaiacol-rich phase divided by the mass fraction of the same compound in the alkane-rich phase. Thus, the selectivity (S), shown in Equation 12, is calculated as the distribution factor of guaiacol divided by the distribution factor of the extracting solvent. These parameters are given by:

$$D_{w,i} = \frac{w_i^a}{w_i^\beta} \tag{11}$$

$$S = \frac{D_{\text{aromatic}}}{D_{\text{alkane}}} = \frac{w^a_{\text{guaiacol}}/w^\beta_{\text{guaiacol}}}{w^a_{\text{alkane}}/w^\beta_{\text{alkane}}} \tag{12}$$

where $w_i^{\alpha or \beta}$ is the mass fraction of compound i in the α or β phase, calling α as the guaiacol rich phase and β as the alkane rich phase. A good solvent for extracting guaiacol has to show a very low distribution ratio compared with the guaiacol for increasing the selectivity. A high distribution ratio of the aromatics allows the use of less solvent in the liquid-liquid extraction. A comparison of the selectivity of three extracting solvents selected in this work, i.e., methanol, ethanol and acetone, are shown in Figure 6. In all of the previous sources is shown that methanol has the best selectivity and distribution ratio compared with the other two solvents and it should be the solvent selected for guaiacol extraction. Figure 7 shows

the experimental selectivity and distribution factor for the guaiacol + dodecane + methanol system at 313.15 K compared with those calculated by NRTL, COSMO-RS and COSMO-SAC. In general, NRTL values are close to the experiments at higher concentrations of guaiacol, but COSMO-RS and COSMO-SAC overestimate $\boldsymbol{D}_{i,w}$ and $\boldsymbol{S}$ mainly because they assume that the alkane-rich is almost pure dodecane or hexadecane, as previously observed in Figure 4.

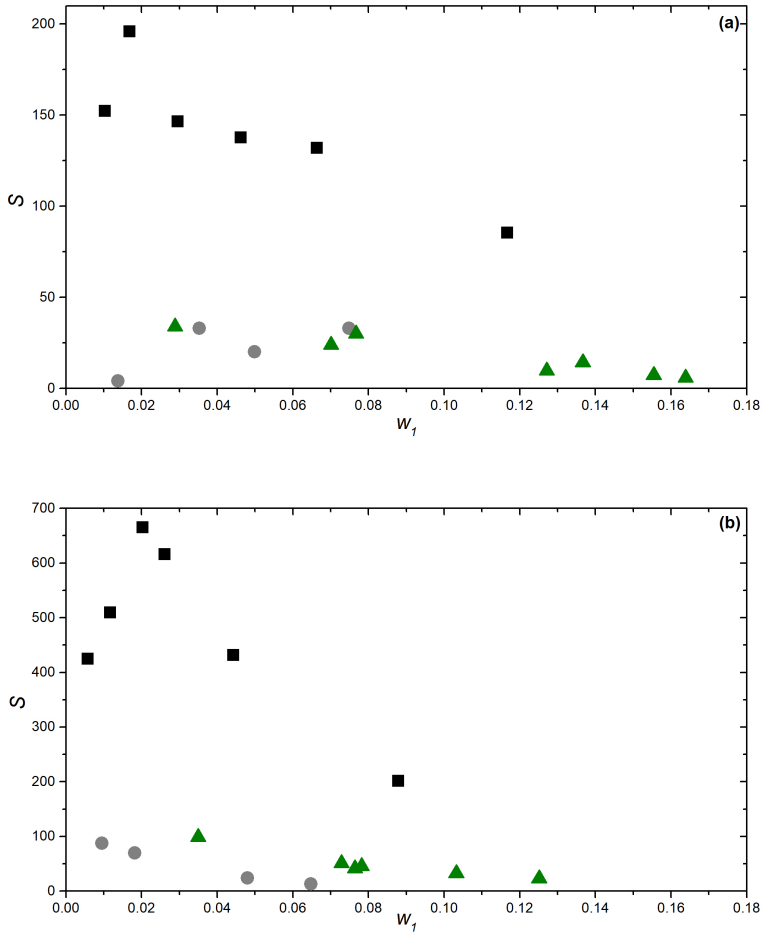

Figure 6: Selectivity of methanol (■), ethanol (▲), and acetone(●) for guaiacol in **(a)** dodecane, and **(b)** hexadecane

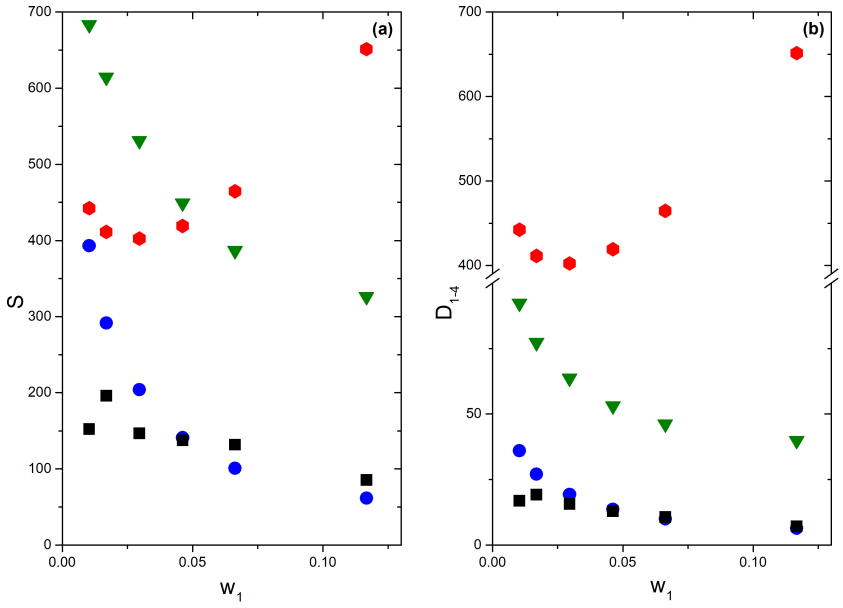

Figure 7: **(a)** selectivity guaiacol + dodecane + methanol and **(b)** capacity guaiacol + methanol at 313.15 K in mass fraction. Experimental data (■), NRTL (●), COSMO-RS (▼) and COSMO-SAC(⬢)

All the distribution factors and selectivities reported in this work are shown in Table A.8 and all of them are compared with the calculated values from NRTL, COSMO-RS and COSMO-SAC in Figure A.2.

Finally, Figure 8 shows the σ-profile in (a) and σ-potential in (b) of the guaiacol and the three extracting solvents involved on this work from COSMO-RS method. The σ-profile of guaiacol is dominated by a series of peaks on the non-polar region. Moreover, it also presents a peak on H-bond acceptor and donor region due to -OH atoms of its alcohol group. This is also shown on the σ-potential figure, where there are exothermic behaviors with both H-bond acceptor and donor groups; i.e. guaiacol is described by COSMO-RS as an amphoteric compound, but with remarkably non-polar features. Therefore, solvents able to extract guaiacol must present the ability to act as H-bond donor and acceptor. This

is the case of ethanol and methanol. Specially, methanol stands out as the best candidate due to its good interaction with guaiacol. Regarding acetone, it presents repulsive behavior with H-bond acceptor groups and weaker attraction with H-bond donor groups, so it does not seem a good candidate for guaiacol extraction based on COSMO-RS calculations.

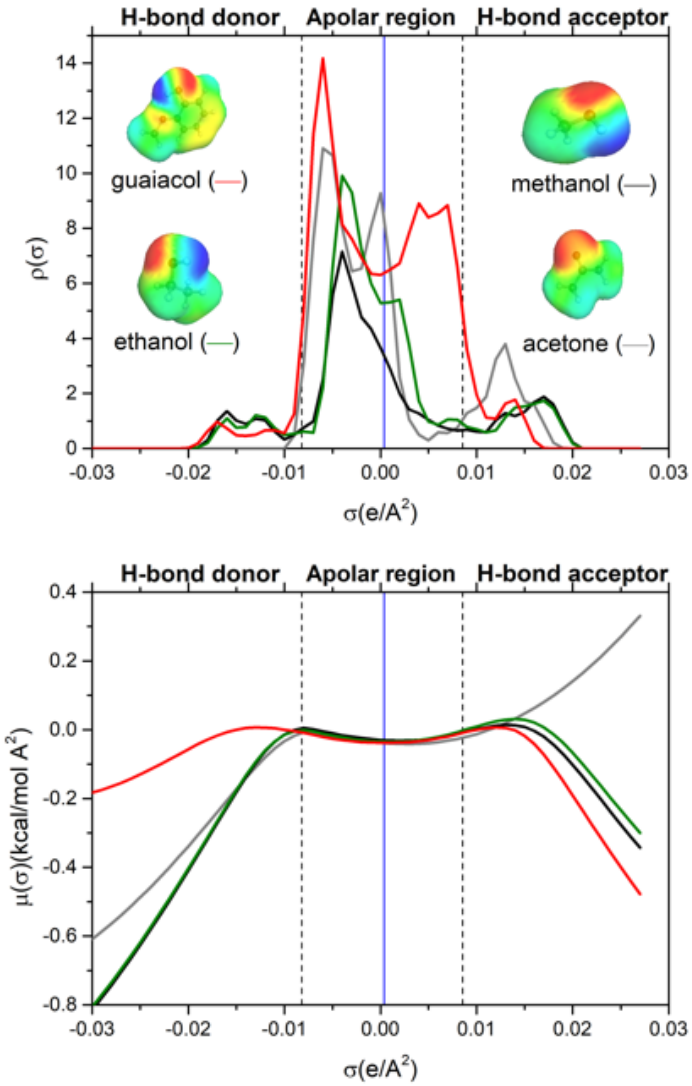

Figure 8: **(a)** sigma profile and **(b)** sigma potential of guaiacol and ots extracting solvents. Red line (-) represent guaiacol, black line (-) methanol, green line (-) ethanol and gray line (-) acetone

5. Conclusions

Three solvents were evaluated for extracting guaiacol from dodecane or hexadecane by liquid-liquid extraction: methanol, ethanol, and acetone. All the compounds involved in the liquid-liquid equilibrium were evaluated in terms of their pure density and viscosity at temperatures between 293.15 K and 333.15 K at 101.3 kPa. Then, the interactions of guaiacol with the three extracting solvents were assessed in terms of the excess volumes showing negative values for all the compositions range, which means a positive interaction of solute + solvent molecules. Also, the viscosities for the same mixtures were evaluated. Then, partial miscibility was observed for the binary pairs composed by guaiacol + dodecane, guaiacol + hexadecane, methanol + dodecane, methanol + hexadecane, and ethanol + hexadecane. All of them present an USCT over 313.15 K. The other binary mixtures were miscible at 313.15 K and 101.3 kPa. Finally, ternary LLE was measured for mixtures composed by guaiacol + (methanol, ethanol, or acetone) + (dodecane or hexadecane) at 313.15 K and 101.3 kPa. All the LLE measurements were modeled with NRTL, COSMO-RS and COSMO-SAC.

In consequence, the densities of guaiacol, methanol, ethanol and acetone are higher than those of dodecane and hexadecane. Then, the upper phase is always alkane-rich and the lower phase mostly guaiacol + extracting solvent. The viscosity of all the compounds is very low, so mass transfer restrictions or equilibrium issues are not expected. The best solvent to extract guaiacol (among those selected for this work) from dodecane and hexadecane is methanol. This fact is supported by the wide immiscibility area formed by the ternary system guaiacol + methanol + (dodecane or hexadecane), the low distribution ratio and high selectivity shown by this compound. Also, σ-profiles and σ-potentials of guaiacol compared with the extracting solvents show that the best interaction with guaiacol occurs with methanol. Ethanol and acetone have several issues. For instance, they are miscible

with dodecane and hexadecane at most of the conditions of temperature and compositions reported. Thus, they cannot extract guaiacol if it is present at low concentrations in the alkane.

Finally, the ternary system guaiacol + methanol + (dodecane or hexadecane) are accurately correlated with NRTL and predicted with COSMO-RS and COSMO-SAC. Then, those models are robust for a potential process simulation of the extraction and recovery of guaiacol.

Acknowledgments

We acknowledge the funding from the Millennium Science Initiative of the Chilean Ministry of Economy, Development, and Tourism, through the grant Nuclei on Catalytic Processes towards Sustainable Chemistry (CSC). We also thank the support of CONICYT Chile through the projects PIA CCTE AFB 170007, Fondecyt Regular (Grant Number 1180982), and PCI REDI170207. We are very grateful to Centro de Computacion Cientifica from Universidad Autonoma de Madrid for their computational facilities and the Seed Fund provided by the School of Engineering UC for the international collaboration.

References

[1] X. Lian, Y. Xue, Z. Zhao, G. Xu, S. Han, H. Yu, Progress on upgrading methods of bio-oil: a review, Int. J. Energy Res. 41 (2017) 1798–1816.

[2] M. Garcia-Perez, A. Chaala, H. Pakdel, D. Kretschmer, C. Roy, Characterization of bio-oils in chemical families, Biomass Bioener. 31 (2007) 222–242.

[3] H. BEN, Chapter 9: Upgrade of bio-oil to bio-fuel and bio-chemical, in: Materials for Biofuels, World Scientific, 2014, pp. 229–266.

[4] J. Tao, C. Li, J. Li, B. Yan, G. Chen, Z. Cheng, W. Li, F. Lin, L. Hou, Multi-step separation of different chemical groups from the heavy fraction in biomass fast pyrolysis oil, Fuel Process. Technol. 202 (2020) 106366.

[5] L. Fan, Y. Zhang, S. Liu, N. Zhou, P. Chen, Y. Cheng, M. Addy, Q. Lu, M. M. Omar, Y. Liu, et al., Bio-oil from fast pyrolysis of lignin: Effects of process and upgrading parameters, Bioresour. Technol. 241 (2017) 1118–1126.

[6] D. E. Resasco, S. P. Crossley, Implementation of concepts derived from model compound studies in the separation and conversion of bio-oil to fuel, Catal. Today 257 (2015) 185–199.

[7] P. M. Mortensen, J.-D. Grunwaldt, P. A. Jensen, K. Knudsen, A. D. Jensen, A review of catalytic upgrading of bio-oil to engine fuels, Appl. Catal., A 407 (2011) 1–19.

[8] A. Sulman, P. Mäki-Arvela, L. Bomont, M. Alda-Onggar, V. Fedorov, V. Russo, K. Eränen, M. Peurla, U. Akhmetzyanova, L. Skuhrovcová, et al., Kinetic and thermodynamic analysis of guaiacol hydrodeoxygenation, Catal. Lett. 149 (2019) 2453–2467.

[9] P. Mäki-Arvela, D. Y. Murzin, Hydrodeoxygenation of lignin-derived phenols: From fundamental studies towards industrial applications, Catalysts 7 (2017) 265.

[10] E. Blanco, C. Sepulveda, K. Cruces, J. García-Fierro, I. Ghampson, N. Escalona, Conversion of guaiacol over metal carbides supported on activated carbon catalysts, Catal. Today (2019).

[11] C. Alvarez, K. Cruces, R. Garcia, C. Sepulveda, J. Fierro, I. Ghampson, N. Escalona, Conversion of guaiacol over different re active phases supported on ceo2-al2o3, Appl. Catal., A 547 (2017) 256–264.

[12] K. Leiva, R. Garcia, C. Sepulveda, D. Laurenti, C. Geantet, M. Vrinat, J. Garcia-Fierro, N. Escalona, Conversion of guaiacol over supported reox catalysts: Support and metal loading effect, Catal. Today 296 (2017) 228–238.

[13] A. Dongil, I. Ghampson, R. García, J. Fierro, N. Escalona, Hydrodeoxygenation of guaiacol over ni/carbon catalysts: effect of the support and ni loading, RSC Adv. 6 (2016) 2611–2623.

[14] X. Zhang, H. Ma, S. Wu, W. Jiang, W. Wei, M. Lei, Fractionation of pyrolysis oil derived from lignin through a simple water extraction method, Fuel 242 (2019) 587–595.

[15] X. Li, S. R. Kersten, B. Schuur, Extraction of guaiacol from model pyrolytic sugar stream with ionic liquids, Ind. Eng. Chem. Res. 55 (2016) 4703–4710.

[16] L. Cesari, L. Canabady-Rochelle, F. Mutelet, Extraction of phenolic compounds from aqueous solution using choline bis (trifluoromethylsulfonyl) imide, Fluid Phase Equilib. 446 (2017) 28–35.

[17] C. Stephan, M. Dicko, P. Stringari, C. Coquelet, Liquid-liquid equilibria of water+ solutes (acetic acid/acetol/furfural/guaiacol/methanol/phenol/propanal)+ solvents (isopropyl acetate/toluene) ternary systems for pyrolysis oil fractionation, Fluid Phase Equilib. 468 (2018) 49–57.

[18] H. Renon, J. M. Prausnitz, Local compositions in thermodynamic excess functions for liquid mixtures, AIChE J. 14 (1968) 135–144.

[19] A. Klamt, F. Eckert, Cosmo-rs: a novel and efficient method for the a priori prediction of thermophysical data of liquids, Fluid Phase Equilib. 172 (2000) 43–72.

[20] S.-T. Lin, S. I. Sandler, A priori phase equilibrium prediction from a segment contribution solvation model, Ind. Eng. Chem. Res. 41 (2002) 899–913.

[21] I.-C. Hwang, K.-L. Kim, S.-J. Park, K.-J. Han, Liquid- liquid equilibria for binary system of ethanol+ hexadecane at elevated temperature and the ternary systems of ethanol+ heterocyclic nitrogen compounds+ hexadecane at 298.15 k, J. Chem. Eng 52 (2007) 1919–1924.

[22] A. Klamt, The basic cosmo-rs, COSMO-RS: From Quantum Chemistry to Fluid Phase Thermodynamics and Drug Design. Amsterdam, The Netherlands: Elsevier (2005) 83–107.

[23] S. Wang, S. I. Sandler, C.-C. Chen, Refinement of cosmo- sac and the applications, Ind. Eng. Chem. Res. 46 (2007) 7275–7288.

[24] F. Eckert, A. C. Klamt, Version c2. 1, release 01.11; cosmologic gmbh & co, KG: Leverkusen, Germany (2010).

[25] A. Schäfer, A. Klamt, D. Sattel, J. C. Lohrenz, F. Eckert, Cosmo implementation in turbomole: Extension of an efficient quantum chemical code towards liquid systems, Phys. Chem. Chem. Phys. 2 (2000) 2187–2193.

[26] D. L. Cunha, J. A. Coutinho, J. L. Daridon, R. A. Reis, M. L. Paredes, Experimental densities and speeds of sound of substituted phenols and their modeling with the prigogine–flory–patterson model, J. Chem. Eng Data 58 (2013) 2925–2931.

[27] F. M. Jaeger, Über die temperaturabhängigkeit der molekularen freien oberflächenenergie von flüssigkeiten im temperaturbereich von- 80 bis+ 1650 c, Zeitschrift für anorganische und allgemeine Chemie 101 (1917) 1–214.

[28] J. Newton Friend, W. D. Hargreaves, Xvii. viscosities of the di-hydroxy benzenes and some of their derivatives, The London, Edinburgh, and Dublin Philosophical Magazine and Journal of Science 37 (1946) 120–126.

[29] Y. Dai, W. Zhao, H. Sun, Y. Guo, W. Fang, Densities and viscosities of ternary system n-dodecane (1)+ bicyclohexyl (2)+ n-butanol (3) and corresponding binaries at t=(293.15 to 333.15) k, J. Chem. Eng Data 63 (2018) 4052–4060.

[30] J. Zhao, J. Wu, Y. Dai, X. Cheng, H. Sun, Y. Guo, W. Fang, Density, viscosity, and freezing point for four binary systems of n-dodecane or methylcyclohexane mixed with 1-heptanol or cyclohexylmethanol, J. Chem. Eng Data 62 (2017) 643–652.

[31] L. Zhang, Y. Guo, J. Xiao, X. Gong, W. Fang, Density, refractive index, viscosity, and surface tension of binary mixtures of exo-tetrahydrodicyclopentadiene with some n-alkanes from (293.15 to 313.15) k, J. Chem. Eng Data 56 (2011) 4268–4273.

[32] D. J. Luning Prak, B. G. Lee, J. S. Cowart, P. C. Trulove, Density, viscosity, speed of sound, bulk modulus, surface tension, and flash point of binary mixtures of butylbenzene+ linear alkanes (n-decane, n-dodecane, n-tetradecane, n-hexadecane, or n-heptadecane) at 0.1 mpa, J. Chem. Eng Data 62 (2016) 169–187.

[33] H. Liu, L. Zhu, Excess molar volumes and viscosities of binary systems of butylcyclohexane with n-alkanes (c7 to c14) at t= 293.15 k to 313.15 k, J. Chem. Eng Data 59 (2014) 369–375.

[34] F. Sirbu, D. Dragoescu, A. Shchamialiou, T. Khasanshin, Densities, speeds of sound, refractive indices, viscosities and their related thermodynamic properties for n-hexadecane+ two aromatic hydrocarbons binary mixtures at temperatures from 298.15 k to 318.15 k, J. Chem. Thermodyn 128 (2019) 383–393.

[35] D. J. L. Prak, B. H. Morrow, S. Maskey, J. A. Harrison, J. S. Cowart, P. C. Trulove, Densities, speeds of sound, and viscosities of binary mixtures of an n-alkylcyclohexane (n-propyl-, n-pentyl-, n-hexyl-, n-heptyl, n-octyl-, n-nonyl-, n-decyl-, and n-dodecyl-) with n-hexadecane, J. Chem. Eng Data 63 (2018) 4632–4648.

[36] M. A. Aissa, I. R. Radović, M. L. Kijevčanin, A systematic study on volumetric and transport properties of binary systems 1-propanol+ n-hexadecane, 1-butanol+ n-hexadecane and 1-propanol+ ethyl oleate at different temperatures: Experimental and modeling, Fluid Phase Equilib. 473 (2018) 1–16.

[37] X. Wang, X. Wang, H. Lang, Measurement and correlation of density and viscosity of n-hexadecane with three fatty acid ethyl esters, J. Chem. Thermodyn 97 (2016) 127–134.

[38] J. Esteban, H. Murasiewicz, T. A. Simons, S. Bakalis, P. J. Fryer, Measuring the density, viscosity, surface tension, and refractive index of binary mixtures of cetane with solketal, a novel fuel additive, Energ. Fuel 30 (2016) 7452–7459.

[39] B. Long, Y. Ding, Probing the intermolecular attractive interactions of binary mixtures of formic acid+ methanol or water via volumetric studies, J. Mol. Liq. 206 (2015) 137–144.

[40] G. Gonfa, M. A. Bustam, N. Muhammad, S. Ullah, Density and excess molar volume of binary mixture of thiocyanate-based ionic liquids and methanol at temperatures 293.15–323.15 k, J. Mol. Liq. 211 (2015) 734–741.

[41] M. A. Varfolomeev, K. V. Zaitseva, I. T. Rakipov, B. N. Solomonov, W. Marczak, Speed of sound, density, and related thermodynamic excess properties of binary mix-

tures of butan-2-one with c1–c4 n-alkanols and chloroform, J. Chem. Eng Data 59 (2014) 4118–4132.

[42] C. Smyth, W. Stoops, The dielectric polarization of liquids. vi. ethyl iodide, ethanol, normal-butanol and normal-octanol, J. Am. Chem. Soc. 51 (1929) 3312–3329.

[43] M. Khimenko, A. VV, G. NN, Polarization and molecular radii of pure liquids, 1973.

[44] Y. Tashima, Y. Arai, Densities of some alcohols and water containing calcium chloride in the region 20-70 c. relation with salt effect on vapor-liquid equilibria, Mem Fac Eng Kyushu Univ 41 (1981) 217–232.

[45] A. Estrada-Baltazar, A. De León-Rodríguez, K. R. Hall, M. Ramos-Estrada, G. A. Iglesias-Silva, Experimental densities and excess volumes for binary mixtures containing propionic acid, acetone, and water from 283.15 k to 323.15 k at atmospheric pressure, J. Chem. Eng Data 48 (2003) 1425–1431.

[46] S. Enders, H. Kahl, J. Winkelmann, Surface tension of the ternary system water+ acetone+ toluene, J. Chem. Eng Data 52 (2007) 1072–1079.

[47] J. Krakowiak, Apparent molar volumes and compressibilities of tetrabutyl-ammonium bromide in organic solvents, J. Chem. Thermodyn 43 (2011) 882–894.

[48] N. Saha, B. Das, D. K. Hazra, Viscosities and excess molar volumes for acetonitrile+ methanol at 298.15, 308.15, and 318.15 k, J. Chem. Eng. Data 40 (1995) 1264–1266.

[49] M. A. Rauf, G. H. Stewart, Viscosities and densities of binary mixtures of 1-alkanols from 15 to 55. degree. c, J. Chem. Eng. Data 28 (1983) 324–328.

[50] S. Mikhail, W. Kimel, Densities and viscosities of methanol-water mixtures., J. Chem. Eng. Data 6 (1961) 533–537.

[51] B. N. Misra, Y. Varshni, Viscosity-temperature relation for solutions., J. Chem. Eng. Data 6 (1961) 194–196.

[52] E. Tommila, E. Lindell, V. ML, R. Laakso, Densities viscosities surface tensions dielectric constants vapour pressures activities and heats of mixing of supholane-water sulpholane-methanol and sulpholane-ethanol mixtures, Suomen Kemistilehti 42 (1969) 95.

[53] B. Garcia, C. Herrera, J. M. Leal, Shear viscosities of binary liquid mixtures: 2-pyrrolidinone with 1-alkanols, J. Chem. Eng. Data 36 (1991) 269–274.

[54] L.-P. Yang, T.-L. Luo, H.-L. Lian, G.-J. Liu, Density and viscosity of (2, 2-dichloro-n, n-di-2-propenylacetamide+ acetone) and (2, 2-dichloro-n, n-di-2-propenylacetamide+ ethanol) at t=(278.15 to 313.15) k, J. Chem. Eng Data 55 (2009) 1364–1367.

[55] K. S. Howard, F. P. Pike, Viscosities and densities of acetone-benzene and acetone-acetic acid systems up to their normal boiling points., J. Chem. Eng. Data 4 (1959) 331–333.

[56] L. Zhang, Y. Guo, J. Xiao, X. Gong, W. Fang, Density, refractive index, viscosity, and surface tension of binary mixtures of exo-tetrahydrodicyclopentadiene with some n-alkanes from (293.15 to 313.15) k, J. Chem. Eng Data 56 (2011) 4268–4273.

[57] N. F. Gajardo-Parra, M. J. Lubben, J. M. Winnert, Á. Leiva, J. F. Brennecke, R. I. Canales, Physicochemical properties of choline chloride-based deep eutectic solvents and excess properties of their pseudo-binary mixtures with 1-butanol, J. Chem. Thermodyn 133 (2019) 272–284.

[58] N. F. Gajardo-Parra, M. I. Campos-Franzani, A. Hernández, N. Escalona, R. I. Canales, Density and viscosity of binary mixtures composed of anisole

with dodecane, hexadecane, decalin, or 1,4-dioxane: Experiments and modeling, J. Chem. Eng 0 (0) null. URL: https://doi.org/10.1021/acs.jced.9b01159. doi:10.1021/acs.jced.9b01159. arXiv:https://doi.org/10.1021/acs.jced.9b01159.

[59] A. Ksiaczak, J. J. Kosinski, Liquid-liquid equilibrium in binary polar aromatic+ hydrocarbon systems, Fluid Phase Equilib. 59 (1990) 291–308.

[60] L. M. Casás, A. Touriño, B. Orge, G. Marino, M. Iglesias, J. Tojo, Thermophysical properties of acetone or methanol+ n-alkane (c9 to c12) mixtures, J. Chem. Eng Data 47 (2002) 887–893.

[61] M. Rogalski, R. Stryjek, Mutual solubility of binary n-hexadecane and polar compound systems, BULLETIN DE L ACADEMIE POLONAISE DES SCIENCES-SERIE DES SCIENCES CHIMIQUES 28 (1980) 139–147.

[62] R. Stryjek, M. Luszczyk, A. Fedorko, Correlation of binary liquid-liquid equilibria, Bull. Pol. Acad. Sci., Tech. Sci. 29 (1981) 203–211.

[63] U. Dahlmann, G. M. Schneider, (liquid+ liquid) phase equilibria and critical curves of (ethanol+ dodecane or tetradecane or hexadecane or 2, 2, 4, 4, 6, 8, 8-heptamethylnonane) from 0.1 mpa to 120.0 mpa, J. Chem. Thermodyn. 21 (1989) 997–1004.

[64] J. Peleteiro, J. Troncoso, D. González-Salgado, J. Valencia, C. Cerdeirina, L. Romani, Anomalous excess heat capacities of ethanol+ alkane mixtures, Int. J. Thermophys. 25 (2004) 787–803.

[65] H. T. French, A. Richards, R. Stokes, Thermodynamics of the partially miscible system ethanol+ hexadecane, J. Chem. Thermodyn. 11 (1979) 671–686.

[66] U. Messow, U. Doye, S. Kuntzsch, D. Kuchenbecker, Thermodynamische untersuchngen an loesungsmittel/n-paraffin-systemen. v. die systeme aceton/n-decan, aceton/n-dodecan, aceton/n/-tetradecan und aceton/n-hexadecan, Z. Phys. Chem. 258 (1977) 90–96.

[67] H. Matsuda, K. Ochi, Liquid–liquid equilibrium data for binary alcohol+ n-alkane (c10–c16) systems: methanol+ decane, ethanol+ tetradecane, and ethanol+ hexadecane, Fluid Phase Equilib. 224 (2004) 31–37.

Appendix A. Supporting information

Appendix A.1. Supporting Tables

Table A.1: Densities (g·cm^{-3}) and viscosities (mPa·s) of guaiacol, dodecane, hexadecane, methanol, ethanol and acetone at different temperatures (K) and a pressure of 101.3 kPa.

	293.15 K	303.15 K	313.15 K	323.15 K	333.15 K
			Density (g·cm^{-3})		
guaiacol	1.1330*	1.1234*	1.1137	1.1039	1.0941
dodecane	0.7488	0.7416	0.7343	0.7270	0.7197
hexadecane	0.7734	0.7665	0.7596	0.7527	0.7458
methanol	0.7913	0.7819	0.7724	0.7627	0.7529
ethanol	0.7894	0.7808	0.7730	0.7632	0.7540
acetone	0.7900	0.7785	0.7669	0.7550	[a]
			Viscosity (mPa·s)		
guaiacol	6.803*	4.505*	3.215	2.424	1.904
dodecane	1.487	1.246	1.062	0.919	0.806
hexadecane	3.419	2.709	2.202	1.828	1.544
methanol	0.586	0.511	0.450	0.400	0.357
ethanol	1.195	0.991	0.828	0.699	0.593
acetone	0.336	0.310	0.288	0.269	[a]

Standard uncertainties u are $u(T)$=0.03 K, $u(P)$= 1 kPa, $u(\rho)$=0.0005 g·cm^{-3} and relative standard uncertainties $u_r(\eta)$=0.06.

[a] above boiling point

* below metling temperature (metaestable)

Table A.2: Parameters adjusted for calculating densities of the pure compounds with Equation 6 and the respective RMSD of the correlation

	a	b	R^2	RMSD
dodecane	0.96300	-0.00073	0.999	0.00014
hexadecane	0.97642	-0.00069	0.999	0.00074
guaiacol	1.41931	-0.00097	0.999	0.00191
methanol	1.07368	-0.00096	0.999	0.00084
ethanol	1.04937	-0.00088	0.998	0.00181
acetone	1.13235	-0.00116	0.999	0.00231

Table A.3: Viscosity fitting coefficients from VFT Equation 7 of pure compounds used in this work and the RMSD of the correlation

	A	B	T_0	RMSD
guaiacol	0.1017	387.2103	201.0302	0.0021
dodecane	0.0503	613.6352	112.0040	0.0010
hexadecane	0.0560	686.1781	126.2325	0.0019
methanol	0.0099	1176.2032	4.7478	0.0014
ethanol	0.0014	2339.9988	-53.3301	0.0031
acetone	0.0423	517.8163	43.1726	0.0001

Table A.4: Densities (g·cm^{-3}) and excess volume (cm^3·mol^{-1}) of guaiacol + solvents liquid mixture at different temperatures (K), compositions of guaiacol (x_1) and a pressure of 101.3 kPa.

guaiacol(1) + methanol(4)										
	Density (g·cm^{-3})					Excess molar volume (cm^3·mol^{-1})				
x_1	293.15 K	303.15 K	313.15 K	323.15 K	333.15 K	293.15 K	303.15 K	313.15 K	323.15 K	333.15 K
0.1203	0.8970	0.8876	0.8781	0.8684	0.8585	-0.728	-0.762	-0.794	-0.8261	-0.857
0.2335	0.9647	0.9553	0.9454	0.9358	0.9249	-1.113	-1.159	-1.184	-1.236	-1.221
0.3595	1.0182	1.0086	0.9987	0.9887	0.9786	-1.337	-1.374	-1.410	-1.440	-1.470
0.4745	1.0535	1.0437	1.0338	1.0237	1.0135	-1.368	-1.398	-1.423	-1.445	-1.464
0.6010	1.0821	1.0723	1.0623	1.0522	1.0419	-1.239	-1.257	-1.273	-1.285	-1.295
0.7218	1.1025	1.0927	1.0827	1.0727	1.0625	-0.987	-0.997	-1.005	-1.009	-1.012
0.8396	1.1177	1.1079	1.0980	1.0881	1.0780	-0.632	-0.636	-0.638	-0.637	-0.637
0.9363	1.1276	1.1179	1.1081	1.0982	1.0883	-0.269	-0.271	-0.271	-0.269	-0.268
guaiacol(1) + ethanol(5)										
	Density (g·cm^{-3})					Excess molar volume (cm^3·mol^{-1})				
x_1	293.15 K	303.15 K	313.15 K	323.15 K	333.15 K	293.15 K	303.15 K	313.15 K	323.15 K	333.15 K
0.1204	0.8703	0.8613	0.8521	0.8427	0.8331	-0.789	-0.800	-0.748	-0.814	-0.819
0.2398	0.9336	0.9243	0.9147	0.9049	0.8949	-1.243	-1.251	-1.203	-1.257	-1.257
0.3598	0.9843	0.9746	0.9648	0.9548	0.9445	-1.441	-1.443	-1.395	-1.433	-1.426
0.4808	1.0252	1.0154	1.0053	0.9952	0.9849	-1.427	-1.422	-1.375	-1.398	-1.385
0.6008	1.0585	1.0486	1.0386	1.0284	1.0181	-1.287	-1.278	-1.238	-1.251	-1.236
0.7199	1.0871	1.0771	1.0671	1.0570	1.0468	-1.138	-1.128	-1.098	-1.106	-1.094
0.8394	1.1083	1.0985	1.0885	1.0785	1.0685	-0.637	-0.631	-0.610	-0.610	-0.599
0.9612	1.1276	1.1179	1.1081	1.0983	1.0884	-0.166	-0.163	-0.157	-0.156	-0.153
guaiacol(1) + acetone(6)										
	Density (g·cm^{-3})					Excess molar volume (cm^3·mol^{-1})				
x_1	293.15 K	303.15 K	313.15 K	323.15 K	333.15 K	293.15 K	303.15 K	313.15 K	323.15 K	333.15 K
0.1199	0.8566	0.8456	0.8344	0.8230	0.8115	-0.764	-0.850	-0.918	-0.993	*
0.2404	0.9144	0.9037	0.8928	0.8818	0.8707	-1.295	-1.387	-1.487	-1.596	*
0.3607	0.9638	0.9534	0.9427	0.932	0.9211	-1.295	-1.388	-1.487	-1.597	*
0.4802	1.0064	0.9961	0.9857	0.9751	0.9644	-1.599	-1.69	-1.742	-1.857	*
0.6002	1.0432	1.0330	1.0227	1.0123	1.0018	-1.468	-1.541	-1.618	-1.705	*
0.7179	1.0743	1.0643	1.0541	1.0439	1.0335	-1.188	-1.240	-1.295	-1.358	*
0.8400	1.1022	1.0923	1.0823	1.0722	1.0621	-0.751	-0.780	-0.812	-0.848	*
0.9538	1.1250	1.1153	1.1055	1.0957	1.0858	-0.265	-0.275	-0.284	-0.296	*

Standard uncertainties u are $u(T)$=0.01 K, $u(P)$= 1 kPa and $u(\rho)$=0.0005 g·cm^{-3}.

Combined expanded uncertainties $U_c(x_1)$=0.002 and $U_c(V^E)$=0.08 cm^{-3}·mol^{-1} with a 0.95 level of confidence.

* above boiling point

Table A.5: Redlich-Kister polynomial fitting coefficients (C_0, C_1, C_2 and C_3) from Equation 9 for the excess volume of guaiacol + solvent with their RMSD at different temperatures (K) and a pressure of 101.3 kPa.

guaiacol(1)+methanol(4)					
T/(K)	C_0	C_1	C_2	C_3	RMSD
293.15	-5.391	1.288	-0.629	0.343	0.006
303.15	-5.495	1.449	-0.752	0.379	0.005
313.15	-5.589	1.617	-0.860	0.438	0.010
323.15	-5.672	1.777	-0.955	0.517	0.005
333.15	-5.738	1.944	-1.097	0.579	0.022
guaiacol(1)+ethanol(5)					
T/(K)	C_0	C_1	C_2	C_3	RMSD
293.15	-5.746	1.169	-0.845	1.145	0.034
303.15	-5.722	1.251	-0.939	1.179	0.033
313.15	-5.553	1.204	-0.714	0.895	0.035
323.15	-5.631	1.357	-1.079	1.343	0.035
333.15	-5.577	1.407	-1.157	1.390	0.035
guaiacol(1)+acetone(6)					
T/(K)	C_0	C_1	C_2	C_3	RMSD
293.15	-6.334	1.264	-0.353	-0.153	0.009
303.15	-6.685	1.520	-0.461	-0.129	0.010
313.15	-7.059	1.796	-0.561	-0.143	0.010
323.15	-7.473	2.085	-0.686	-0.131	0.010

Table A.6: Viscosities (mPa·s) of guaiacol (1) + solvent liquid mixture at different temperatures (K), compositions of guaiacol (x_1) and solvents a pressure of 101.3 kPa.

guiacol(1) + methanol(4)					
	Viscosity (mPa·s)				
x_1	293.15 K	303.15 K	313.15 K	323.15 K	333.15 K
0.121	1.097	0.911	0.768	0.654	0.562
0.233	1.450	1.172	0.961	0.803	0.680
0.360	2.894	2.147	1.649	1.308	1.063
0.475	4.044	2.865	2.134	1.647	1.316
0.601	5.120	3.479	2.514	1.906	1.498
0.722	5.860	3.898	2.850	2.139	1.667
0.840	6.580	4.321	3.059	2.291	1.790
0.935	6.866	4.517	3.201	2.396	1.877
guiacol(1) + ethanol(5)					
	Viscosity (mPa·s)				
x_1	293.15 K	303.15 K	313.15 K	323.15 K	333.15 K
0.120	1.713	1.368	1.108	0.912	0.759
0.240	2.410	1.839	1.440	1.156	0.944
0.360	3.242	2.374	1.803	1.413	1.135
0.481	4.158	2.938	2.175	1.673	1.327
0.601	5.036	3.445	2.502	1.896	1.491
0.720	5.730	3.840	2.753	2.074	1.626
0.839	6.292	4.177	2.975	2.238	1.752
0.961	6.701	4.432	3.154	2.376	1.863
guaiacol(1) + acetone(6)					
	Viscosity (mPa·s)				
x_1	293.15 K	303.15 K	313.15 K	323.15 K	333.15 K
0.126	2.008	1.681	1.428	1.230	1.072
0.235	1.742	1.469	1.258	1.091	0.956
0.338	1.523	1.314	1.128	0.986	0.871
0.433	1.413	1.203	1.041	0.920	0.807
0.574	1.264	1.083	0.941	0.829	0.737
0.668	1.200	1.029	0.898	0.793	0.707
0.774	1.131	0.973	0.850	0.752	0.671
0.893	1.088	0.937	0.818	0.724	0.646

Standard uncertainties u are $u(T)$=0.01 K, $u(P)$= 1 kPa.

Combined standard uncertainties $U_c(\mathrm{x}_1)$=0.002 with a 0.95 level of confidence. Relative standard uncertainties $u_r(\eta)$=0.06

Table A.7: Experimental liquid-liquid equilibrium data, in weight fraction, for the binary system of guaiacol + solvent at different temperatures and 101.3 kPa

guaiacol(1) + dodecane(2)				
	alkane rich phase		guaiacol rich phase	
T (K)	w_1	w_2	w_1	w_2
293.15	0.1089	0.8911	0.9467	0.0533
303.15	0.1441	0.8559	0.9300	0.0700
313.15	0.2030	0.7970	0.9156	0.0844
323.15	0.2931	0.7069	0.8890	0.1110
328.15	0.4081	0.5919	0.8546	0.1454
guaiacol(1) + hexadecane(3)				
	alkane rich phase		guaiacol rich phase	
T (K)	w_1	w_3	w_1	w_3
293.15	0.0689	0.9311	0.9684	0.0316
303.15	0.0941	0.9059	0.9550	0.0450
313.15	0.1318	0.8682	0.9395	0.0605
323.15	0.1790	0.8210	0.9142	0.0858
333.15	0.2462	0.7538	0.9011	0.0989
338.15	0.3003	0.6997	0.8956	0.1044
dodecane(2) + methanol (4)				
	alkane rich phase		guaiacol rich phase	
T (K)	w_2	w_4	w_2	w_4
293.15	0.9881	0.0118	0.0686	0.9313
303.15	0.9859	0.0140	0.0832	0.9168
313.15	0.9825	0.0175	0.0515	0.9486
323.15	0.9856	0.0144	0.1153	0.8847
333.15	0.9706	0.0294	0.1478	0.8522
hexadecane(3) + methanol (4)				
	alkane rich phase		guaiacol rich phase	
T (K)	w_3	w_4	w_3	w_4
293.15	0.9942	0.0058	0.0303	0.9697
303.15	0.9925	0.0075	0.0377	0.9623
313.15	0.9941	0.0059	0.0235	0.9765
323.15	0.9899	0.0101	0.0552	0.9448
333.15	0.9838	0.0162	0.0758	0.9242

Standard uncertainties u are $u(T)$=0.05 K, $u(w)$= 0.005

Table A.8: Experimental liquid-liquid equilibrium data, in weight fraction, distribution factors and selectivities for the ternary system of guaiacol + alkane + solvent at 313.15 K and 101.3 kPa

guaiacol(1) + dodecano(2) + methanol(4)								
alkane rich phase			guaiacol rich phase					
w_1	w_2	w_4	w_1	w_2	w_4	D_1	D_2	$S_{1,2}$
0.00000	0.98252	0.01748	0.00000	0.05145	0.94855			
0.01028	0.97195	0.01777	0.17356	0.10771	0.71873	16.88499	0.11082	152.36392
0.01683	0.96807	0.01510	0.32395	0.09514	0.58091	19.24955	0.09827	195.87834
0.02956	0.96163	0.00880	0.46349	0.10282	0.43368	15.67823	0.10693	146.62754
0.04621	0.94837	0.00542	0.59609	0.08884	0.31507	12.90024	0.09367	137.71866
0.06631	0.92582	0.00786	0.70598	0.07469	0.21933	10.64603	0.08067	131.97105
0.11669	0.87705	0.00626	0.82861	0.07287	0.09852	7.10083	0.08308	85.46844
0.20699	0.79301	0.00000	0.90040	0.09960	0.00000			
guaiacol(1) + hexadecane(3) + methanol(4)								
alkane rich phase			guaiacol rich phase					
w_1	w_3	w_4	w_1	w_3	w_4	D_1	D_3	$S_{1,3}$
0.00000	0.99412	0.00588	0.00000	0.02347	0.97653			
0.00574	0.98852	0.00573	0.17230	0.06979	0.75791	30.01742	0.07060	425.17297
0.01164	0.98008	0.00828	0.33219	0.05491	0.61291	28.53866	0.05603	509.38207
0.02029	0.97490	0.00481	0.51850	0.03745	0.44406	25.55446	0.03841	665.23480
0.02610	0.97024	0.00366	0.62393	0.03766	0.33841	23.90536	0.03882	615.87733
0.04428	0.95219	0.00353	0.75398	0.03753	0.20849	17.02755	0.03941	432.01345
0.08783	0.90807	0.00410	0.86068	0.04412	0.09520	9.79939	0.04859	201.68920
0.13202	0.86798	0.00000	0.93217	0.06783	0.00000			
guaiacol(1) + dodecane(2) + ethanol(4)								
alkane rich phase			guaiacol rich phase					
w_1	w_2	w_5	w_1	w_2	w_5	D_1	D_2	$S_{1,2}$
0.14929	0.71403	0.13668	0.48099	0.16040	0.35861	3.22185	0.22464	14.34225
0.15144	0.72141	0.12715	0.42703	0.20628	0.36669	2.81980	0.28594	9.86150
0.15889	0.68567	0.15544	0.38569	0.22737	0.38695	2.42740	0.33160	7.32021
0.15908	0.77079	0.07013	0.60777	0.12290	0.26933	3.82053	0.15945	23.96116
0.16321	0.76004	0.07675	0.71030	0.11003	0.17967	4.35206	0.14477	30.06217
0.16483	0.67129	0.16388	0.36062	0.25071	0.38868	2.18783	0.37347	5.85804
0.17053	0.80060	0.02887	0.74725	0.10360	0.14915	4.38193	0.12940	33.86265
0.20718	0.79282	0.00000	0.89624	0.10376	0.00000			
guaiacol(1) + hexadecane(3) + ethanol(5)								
alkane rich phase			guaiacol rich phase					
w_1	w_3	w_5	w_1	w_3	w_5	D_1	D_3	$S_{1,3}$
0.05041	0.82447	0.12512	0.23870	0.16901	0.59228	4.73517	0.20499	23.09927
0.06027	0.83651	0.10323	0.32744	0.13824	0.53432	5.43289	0.16526	32.87517
0.06783	0.85572	0.07645	0.39688	0.12116	0.48197	5.85110	0.14159	41.32471
0.07119	0.85062	0.07819	0.42219	0.11134	0.46647	5.93047	0.13089	45.30784
0.07422	0.85291	0.07287	0.46013	0.10359	0.43628	6.19954	0.12145	51.04403
0.10312	0.86189	0.03498	0.78346	0.06618	0.15036	7.59756	0.07678	98.94617
0.13202	0.86798	0.00000	0.93217	0.06783	0.00000	7.06082	0.07815	90.35315
guaiacol(1) + dodecane(2) + acetone(6)								
alkane rich phase			guaiacol rich phase					
w_1	w_2	w_6	w_1	w_2	w_6	D_1	D_2	$S_{1,2}$
0.17150	0.79325	0.03525	0.71979	0.16491	0.11530	4.19703	0.20789	20.18853
0.17336	0.81287	0.01377	0.82459	0.11736	0.05805	4.75652	0.14438	32.94505
0.19697	0.75319	0.04984	0.61063	0.23531	0.15406	3.10012	0.31242	9.92298
0.20718	0.79282	0.00000	0.89624	0.10376	0.00000	4.32590	0.13087	33.05378
0.22788	0.69725	0.07487	0.48859	0.35810	0.15330	2.14407	0.51359	4.17467
guaiacol(1) + hexadecane(3) + acetone(6)								
alkane rich phase			guaiacol rich phase					
w_1	w_3	w_6	w_1	w_3	w_6	D_1	D_3	$S_{1,3}$
0.08971	0.89207	0.01822	0.75828	0.10842	0.13329	8.45257	0.12154	69.54698
0.09180	0.84342	0.06478	0.44347	0.30856	0.24797	4.83083	0.36584	13.20462
0.09527	0.85674	0.04799	0.57124	0.21183	0.21693	5.99601	0.24725	24.25069
0.11257	0.87794	0.00949	0.85645	0.07611	0.06744	7.60815	0.08669	87.76118
0.13202	0.86798	0.00000	0.93217	0.06783	0.00000	7.06082	0.07815	90.35315

Standard uncertainties u are $u(T)$=0.05 K, $u(w)$= 0.005

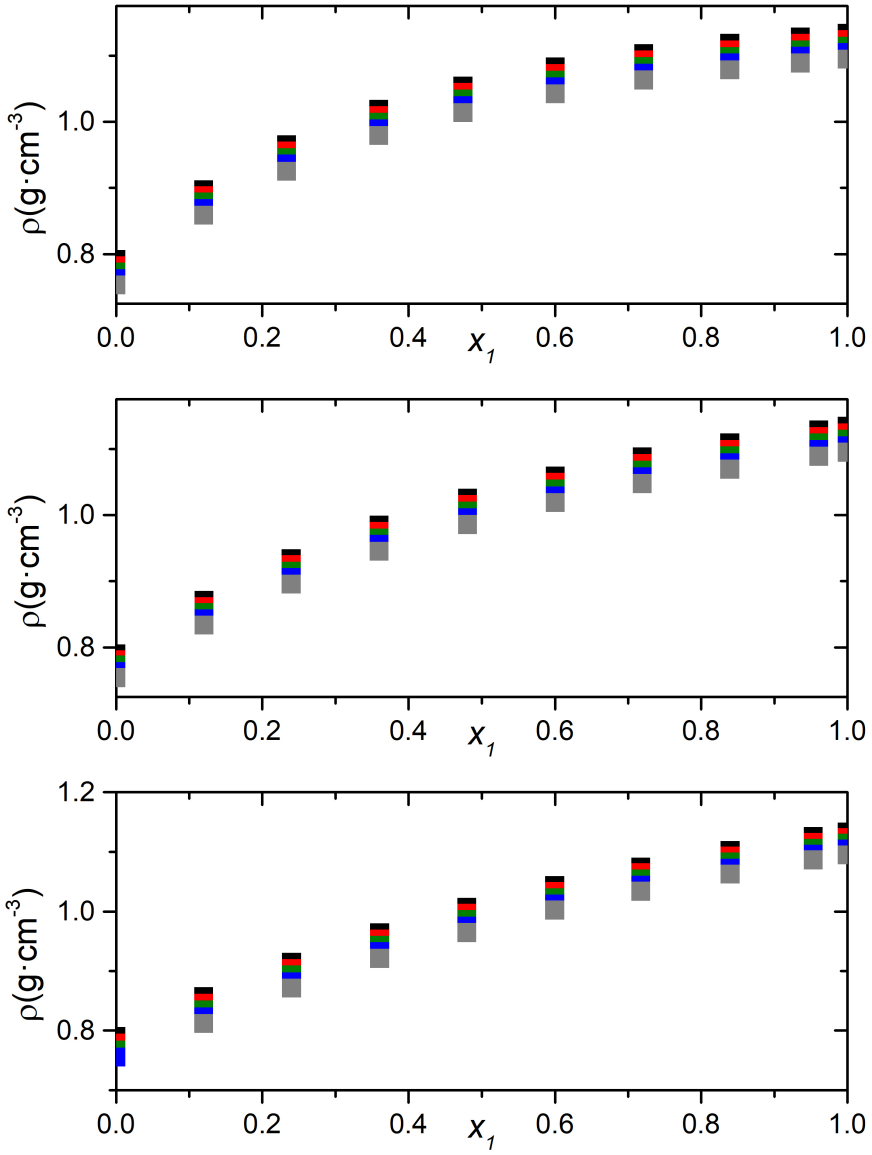

Figure A.1: Density (g·cm^{-3}) in terms of the mole fraction of guaiacol for the binary mixtures composed of **(a)** guaiacol + methanol, **(b)** guaiacol + ethanol and **(c)** guiacol + acetone at a pressure of 101.3 kPa and different temperatures: 293.15 K (■), 303.15 K (■), 313.15 K (■), 323.15 K (■), and 333.15 K (■).

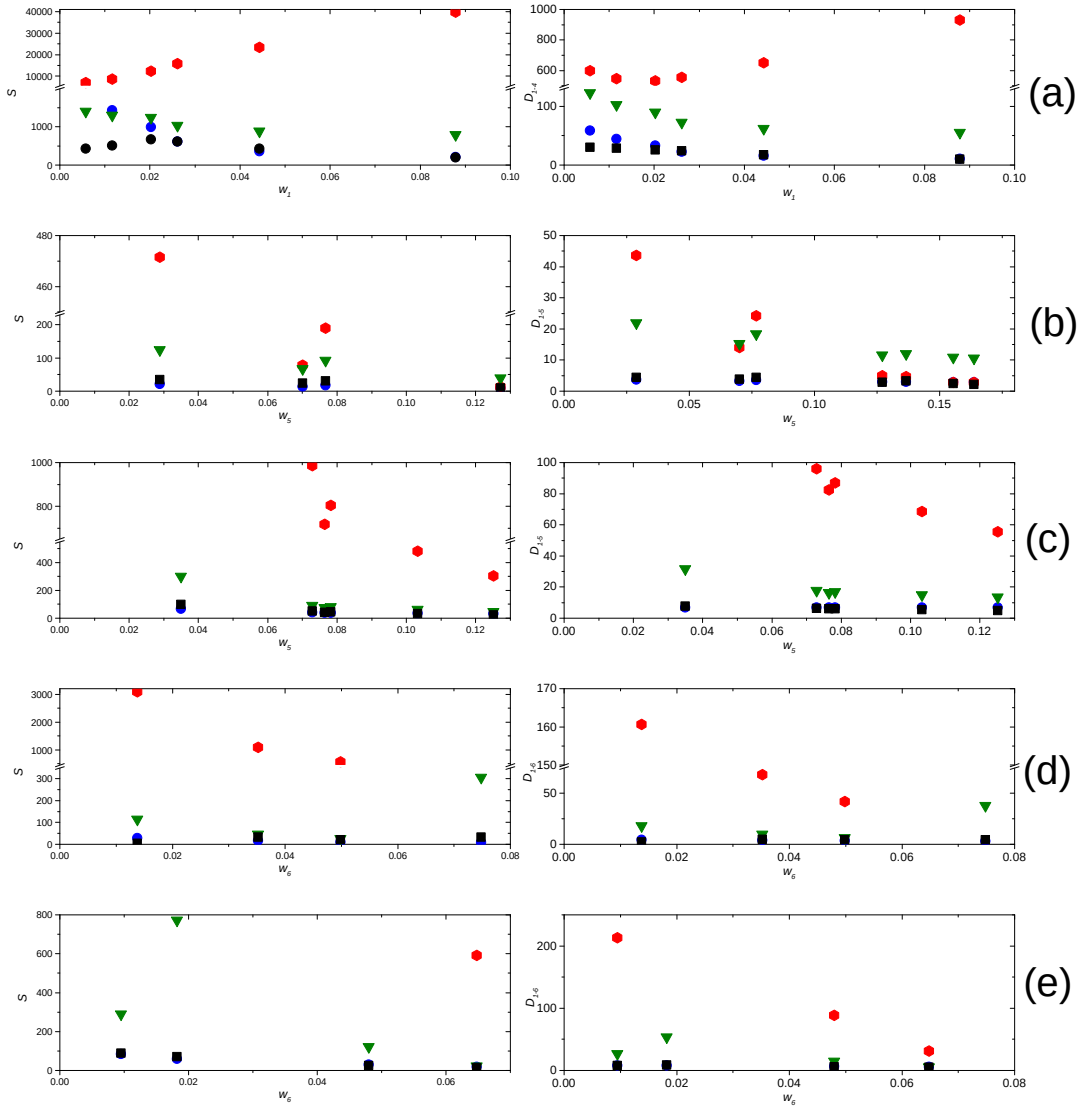

Figure A.2: Selectivity and distribution factor of **(a)** guaiacol + hexadecane + methanol, **(b)** guaiacol + dodecane + ethanol, **(c)** guaiacol + hexadecane + ethanol, **(d)** guaiacol + dodecane + acetone, **(e)** guaiacol + hexadecane + acetone at 313.15 K, in mass fraction and 101.3 kPa. Experimental data (■), NRTL (●), COSMO-RS (▼) and COSMO-SAC(⬢)